RUSSIAN JOURNAL OF EARTH SCIENCES, VOL. 6, NO. 3, PAGES 153–183, JUNE 2004

Intraplate magmatism of the De Long Islands: A response to the propagation of the ultraslow-spreading Gakkel Ridge into the passive continental margin in the Laptev Sea

S. A. Silantyev[1], O. G. Bogdanovskii[2], P. I. Fedorov[3], S. F. Karpenko[1], and Yu. A. Kostitsyn[1]

Abstract. Synthesis of petrological, geochemical, and isotopic data on volcanic rocks and a related suite of xenoliths in the De Long Islands in the eastern sector of the Arctic basin is presented with the aim of reproducing the geochemical nature of the mantle sources of basaltic magmatism and its geodynamic environment in the continental shelf of the Laptev Sea, southeast of its intersection with the southern termination of the Gakkel Ridge. The main tool of this research was the comparative analysis of the isotopic characteristics of magmatic products on islands of this archipelago situated at different distances from the oceanic margin of the shelf. The reconstructed magmatic evolution at De Long Islands implies its close relations with the activity of a plume mantle source that occurred beneath the continental shelf of the Laptev Sea and was responsible for pulses of magmatic activity in this area of the eastern sector of the Arctic over the past 124 m.y. The volcanic activity at De Long Islands is determined to have become systematically younger from the offshore boundary of the continental shelf in the Laptev Sea (Bennett Island) inward the shelf (Zhokhov Islands) and farther southeastward (Vil'kitskii Island).

Introduction

The De Long Archipelago, located in a still poorly studied area in the eastern Arctic sector, consists of five small islands at the seaward margin of the continental shelf in the Laptev Sea (Figure 1). The largest of the islands, which is the closest to the shelf margin, is Bennett Island. Southeast of it, Zhokhov and Vil'kitskii islands make up the central part of the archipelago, and the islands of Jeannette and Henrietta lie in its eastern flank. The geographic setting of the archipelago, which is located near the so-called Pole of Inaccessibility (75°44′–77°07′ N, 148°50′–158°E), predetermined the dramatic history of its discovery and exploring.

The De Long Islands were named after George Washington De Long, a US Navy lieutenant, who headed in 1879 an American expedition aimed to achieve the North Pole. De Long took his yacht "Jeannette" through the Bering Strait and headed northwest. The "Jeannette" was enclosed by the ice, froze in, and drifted in this state for 500 km northwest during 20 months. In the course of this drift, which ended with the crushing of the vessel and its sinking, the islands of Jeannette, Henrietta, and Bennett were discovered. Most participants of the expedition, including De Long himself, died of exposure and starvation when trying to reach Russian settlements in the Siberian Arctic shore near the Lena mouth. In 1902–1915, the islands and surrounding waters were visited by a series of Russian expeditions. During one of them, headed by E. V. Tol', the first rock samples were collected in Bennett Island, but Tol' himself and all his men vanished without a trace, and their rock collection was found later in Bennett Island.

[1] Vernadsky Institute of Geochemistry and Analytical Chemistry, Russian Academy of Sciences, Moscow, Russia
[2] Max-Plank-Institut für Chemie, Postfach 3060, D-55020 Mainz, Germany
[3] Geological Institute, Russian Academy of Sciences, Moscow, Russia

Paper number TJE04154.
ISSN: 1681–1208 (online)

The online version of this paper was published 15 July 2004.
URL: http://rjes.wdcb.ru/v06/tje04150/tje04150.htm

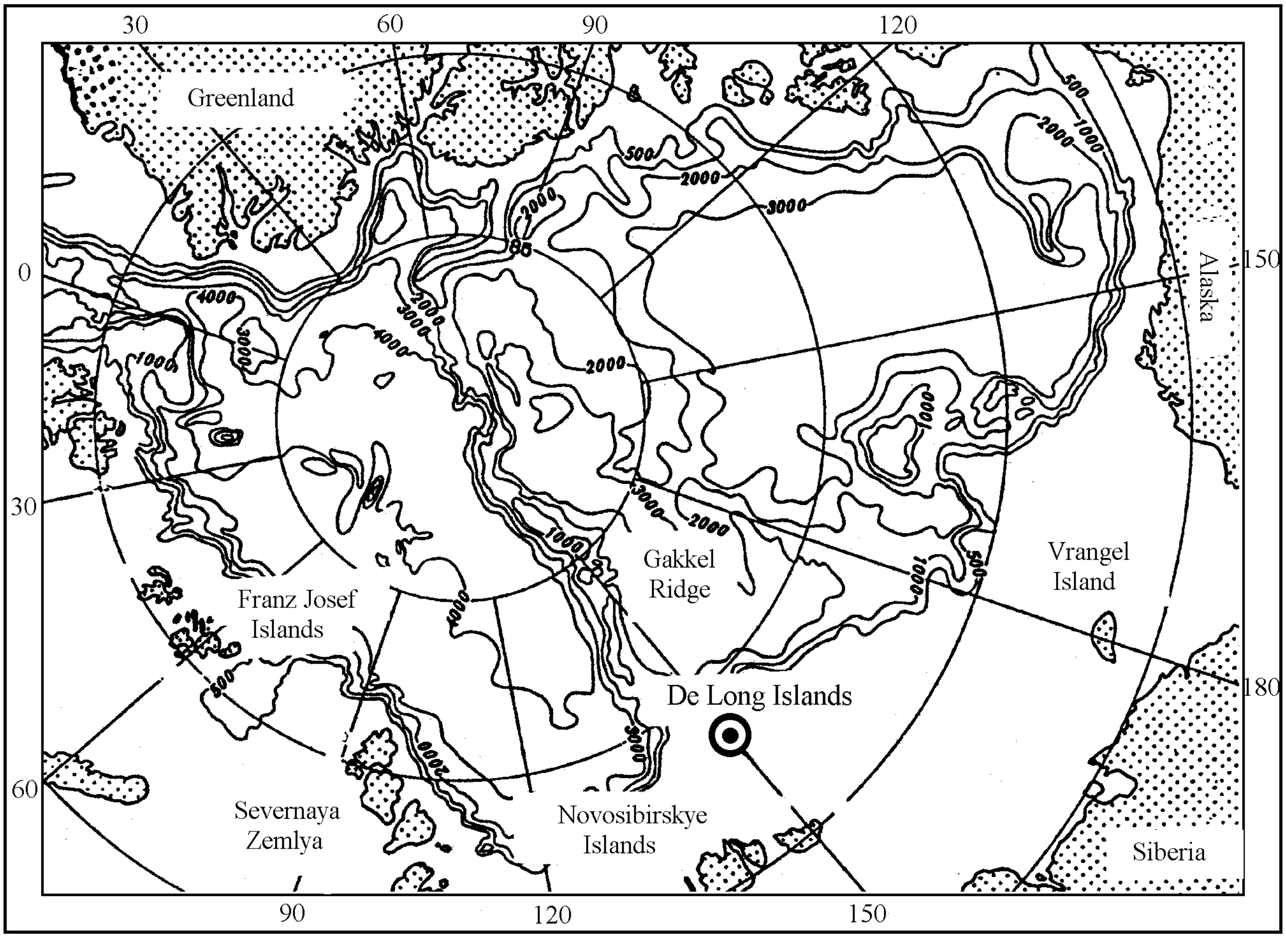

Figure 1. Sketch map of the eastern sector of the Arctic basin and the location of the De Long Islands.

The expedition of two Russian icebreakers "Taymyr" and "Vaigach" (the chief of the 1913–1915 expeditions was B. A. Vil'kitskii, assistant to the chief A. N. Zhokhov), which was launched with the aim of exploring the prospects of using the Northern Sea Route, discovered the islands of Vil'kitskii (1913) and Zhokhov (1915). Later, fieldwork was sporadically conducted on the islands of the archipelago by AANII.

The De Long Islands lie practically exactly on the continuation of the trend axis of the Gakkel mid-oceanic ridge into the passive continental margin of the Laptev Sea shelf, a fact that led Ya. Ya. Gakkel to hypothesize in 1957 that the superstructure of the Mid-Atlantic Ridge (MAR), including the Gackcel Ridge, extends across the North Pole and De Long Islands to the basin of the Indigirka River [*Gakkel,* 1957]. Later geophysical data on this area in the Arctic basin were interpreted [*Naryshkin,* 1987] as indicating that the islands of Zhokhov and Vil'kitskii belong to an extensive submarine plateau, which reaches the continental slope of the Eurasian basin. Mafic magmatic rocks at De Long Islands were dated [*Vol'nov and Sorokov,* 1961; *Vol'nov et al.,* 1970] as Cretaceous and younger. Newly obtained data on the composition and age of volcanics from Bennettt Island were reported in [*Fedorov et al.,* 2002] and used in this paper.

The most exhaustive and systematic information on the composition and age of magmatic rocks and related mantle and crustal xenoliths from the central part of the De Long Islands were presented in a series of publications that synthesized the results of fieldwork on Zhokhov and Vil'kitskii islands conducted in 1986 and 1988 within the scope of the joint high-latitude expedition of Shirshov Institute of Oceanology and Vernadsky Institute of Geochemistry and Analytical Chemistry of the Russian Academy of Sciences [*Bogdanovskii et al.,* 1992, 1993; *Savostin et al.,* 1988; *Silantyev et al.,* 1991, 2002]. The newly obtained data reported in these papers were supplemented with the latest information on magmatic rocks of Bennett Island and used as the basis of this research.

The main cause why we returned to the problem of the geodynamic environment of magmatism at De Long Islands was the obvious breakthrough in the currently adopted concepts of the geology of the Eurasian sector of the Arctic Ocean related to exploring the crest zone of the Gakkel Ridge between 5°W and 85°E conducted by the AMORE international expedition in 2001 aboard the well-equipped icebreaker-class vessels "Polarstern" (Alfred-

Wegener-Institut, Bremenhaven, Germany) and "Healy" (USCGS, Seattle, United States). The results obtained by this expedition provided vast volumes of new geophysical and bathymetric information on the structure of the Gakkel Ridge and, what is particularly important in the context of our research, a large collection of mantle peridotites and basalts from throughout the axial zone of the ridge.

This paper also presents the very first data on the Sr and Nd isotopic composition of basalts from the rock collection sampled at lava flows on Bennett Island, one of the largest islands of the archipelago. When compared with preexisting data on Zhokhov and Vil'kitskii islands, this information makes it possible to reconstruct the geochemical nature of the mantle sources of basaltic magmatism in the continental shelf of the Laptev Sea immediately southeast of its intersection with the southern termination of the Gakkel Ridge. This comparative analysis of the isotopic characteristics of magmatism on the islands of the archipelago is instrumental in reproducing the major stages of intraplate volcanism in the passive continental margin during the gradual propagation of the ultraslow-spreading ridge. It should be mentioned that De Long Islands are among the world's few structures suitable for examining the geodynamic environment of interaction between a so-called "propagating ridge" and a passive continental margin (such as the Red Sea Rift).

We considered it necessary to amend our earlier isotopic data published elsewhere. In our previous research conducted in the 1970s in compliance with the method developed by G. Wasserburg et al. at the California Institute of Technology, the ^{150}Nd/^{142}Nd isotopic ratio was normalized to 0.209647, and, thus, the ^{143}Nd/^{144}Nd ratio for CHUR was assumed equal to 0.511847. The data obtained in the course of this research by modern methods, currently employed at most isotopic laboratories around the world, were based on normalizing the ^{146}Nd/^{144}Nd ratio to 0.7219, which implies the value of the ^{143}Nd/^{144}Nd ratio for CHUR equal to 0.512638. Hence, to compare our earlier data [*Bogdanovskii et al.,* 1992, 1993] with those obtained recently on volcanic rocks from Bennett Island, all of our earlier ^{143}Nd/^{144}Nd ratios were corrected using a coefficient equal to 1.00154. It is pertinent to mention that none of our ^{147}Sm/^{144}Nd ratios has changed.

Geology of De Long Islands

Information available on the geology of the De Long Islands is scarce, almost all of it presented in the classic multivolume publication [*Geology...,* 1970].

Bennett Island. According to the aforementioned publication, Bennett Island is composed of Cretaceous [*Vol'nov and Sorokin,* 1961] or Miocene [*Geology...,* 1984] basalt flows, which rest on compositionally variegated sedimentary rocks. The sedimentary complex consists of Cambrian mudstones with trilobite fossils and Ordovician mudstones and sandstones. The thickness of the olivine basalt flows amounts to approximately 500 m. It has been demonstrated [*Fedorov et al.,* 2002] that the alkaline basalts composing stratified lava sheets on Bennett Island have an age of 106 Ma, while the magnesian basalts composing volcanic cones and lava flows were dated (K–Ar) at 109–124 Ma.

Zhokhov and Vel'kitskii islands. Earlier researchers suggested that both islands are made up of olivine and nepheline basalts [*Backlund,* 1920; *Geology...,* 1970]. The results of our fieldwork in 1986 and 1988 suggest that Zhokhov Island completely consists of basaltoid lava flows (mostly of olivine-phyric varieties). As can be seen in the highest (50 m) exposure in the coastal cliffs in the southeastern portion of Zhokhov Island, there are at least five lava sheets, whose tops are marked with cinderlike rocks of dark gray and reddish brown colors, often with traces of flow. Each of the flows is usually clearly stratified from top to bottom in the following manner: (1) highly porous olivine-phyric basalt, (2) basalt of intermediate porosity, (3) massive basalt with rare olivine crystals, and (4) variolitic basalt. The central, most elevated part of Zhokov Island, which is crowned with a small rocklet (called Devil's Finger), and the area north of it consist of black, reddish, and bright orange volcanic rocks with evidence of explosive genesis (abundant volcanic cinder and fragments of volcanic bombs). The low dome-shaped hillocks in the central part of the island seem to have been eruption centers from which lava flows were outpoured. All varieties of the Zhokov basaltoids contain small (no more than 2×3×5 cm) apple-green xenoliths, which are clearly discernible in the dark gray and black host rocks. These xenoliths resemble mantle xenoliths of lherzolites widespread in areas of intraplate magmatism. Lava flows on the southwestern shore of the island also occasionally contain xenoliths of mafic magmatic rocks and crustal quartzites.

When disembarking at Vil'kitskii Island in May of 1988, the authors of this paper managed to collect samples at an extensive exposure in the southern cliffy shore of this small (10×3 km) island. The central part of the exposure (that extended for about 4.5 km from west to east) was composed of massive basaltoids with very small xenoliths identical to those in the Zhokhov rocks. From east to west, the body of massive basaltoids was surrounded by highly porous lava flows resembling the volcanic rocks in the central part of Zhokhov Island. These porous lavas also contained rare very small xenoliths of apple-green color.

Jeannette and Henrietta islands. The data reported in [*Geology...,* 1970] indicate that the stratigraphic sequence of Henrietta Island comprises three major units: (1) lower, consisting of quartzites and clayey shales (150–200 m); (2) middle, made up of tuffites and diabases (700–900 m); and (3) upper, composed of conglomerates (200–300 m). A similar stratigraphy is also typical of Henrietta Island. The sedimentary complexes of Jeannette and Henrietta islands are of Cretaceous age. A similar age was determined for basalts with pyroxene (augite) phenocrysts that intrude the sedimentary sequence of Henrietta Island.

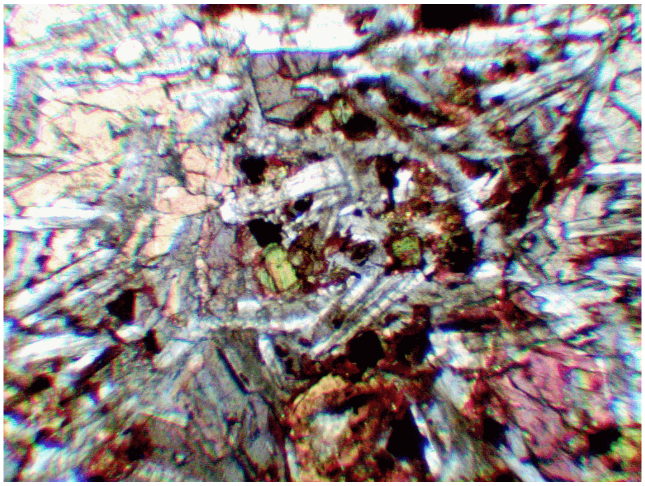

Figure 2. Microphotograph of magnesian alkaline basalt (petrographic thin section) from Bennett Island, sample B833. Crossed polarizers, magnification 72×.

Analytical Techniques

The contents of major and trace elements were determined on a PW-1600 (Philips) XRF spectrometer (analyst T. V. Romashova) at the Central Analytical Laboratory of Vernadsky Institute of Geochemistry and Analytical Chemistry, Russian Academy of Sciences. REE were analyzed in the rocks by neutron activation at the same analytical center. The Nd, Sr, S, C, and O isotopic ratios and the K–Ar age of the alkaline olivine basalts, limburgites, and crustal and mantle xenoliths from Zhokhov and Vil'kitskii islands were discussed in [*Bogdanovskii et al.,* 1992, 1993]. We used data on the contents of major incompatible elements in basalts from Bennett Island and information on the mineralogy of these rocks compiled from [*Fedorov et al.,* 2002].

Minerals in rocks from Zhokhov and Vil'kitskii islands were analyzed by N. N. Kononkova on a CAMEBAX electron microprobe at Vernadsky Institute. The standards were natural and synthetic minerals. The spot analyses were conducted at an accelerating voltage of 15–20 kV and a beam current of 35 mA.

The Sr and Nd isotopic compositions of volcanic rocks from Bennett Island were measured on a TRITON TI multicollector mass spectrometer at the Laboratory of Isotopic Geochemistry of Vernadsky Institute.

Petrographic Outline and Petrology of Magmatic Complexes in Bennett, Zhokhov, and Vil'kitskii Islands

The olivine-phyric basalts from stratified lava flows on Bennett Island have an interstitial texture and consist of devitrified glass, plagioclase microlites, olivine phenocrysts (Mg# = 58–62) and microlites (Mg# = 57-58), and volumetrically subordinate clinopyroxene microlitic phenocrysts and aggregates in the glassy rock matrix (both varieties have Mg# = 57-62). The basaltoids composing cones and related lava flows on Bennett Island are variably altered rocks with a subintersertal texture of the groundmass and phenocrysts of plagioclase, olivine, and clinopyroxene (occurring in subordinate amounts) (Figure 2). The most altered varieties of these rocks contain chlorite and actinolite. Compared with the basalts from the stratified flows, the volcanic rocks of the cones have more magnesian olivine (Mg# equal to 64–74 for phenocrysts and 63–65 for microlites) and clinopyroxene (73–78 for phenocrysts and 69–75 for microlites), with the latter mineral being also more aluminous (Table 1, Figures 3, 4).

The volcanic rocks of Zhokhov Island can be subdivided into three major petrographic groups [*Silantyev et al.,* 1991]. The first group, which is spread most widely, comprises pyroxene-bearing olivine-phyric basalts, whose composed of olivine, clinopyroxene, orthopyroxene, and, sometimes, plagioclase (Figure 5). Some of the olivine- and plagiophyric basalts are holocrystalline rocks with a subdoleritic (microphitic) texture; they usually compose the inner portions of lava flows. The second group consists of volcanic rocks found exclusively in the central part of the island (at Devil's Finger Hill). These rocks are olivine-phyric basalts with rare clino- and orthopyroxene (Figure 6a). The third group of volcanics from Zhokhov Island, which were sampled 3 km northwest of Devil's Finger Hill, includes cinder-like bright orange-brown rocks, perhaps, of explosive genesis.

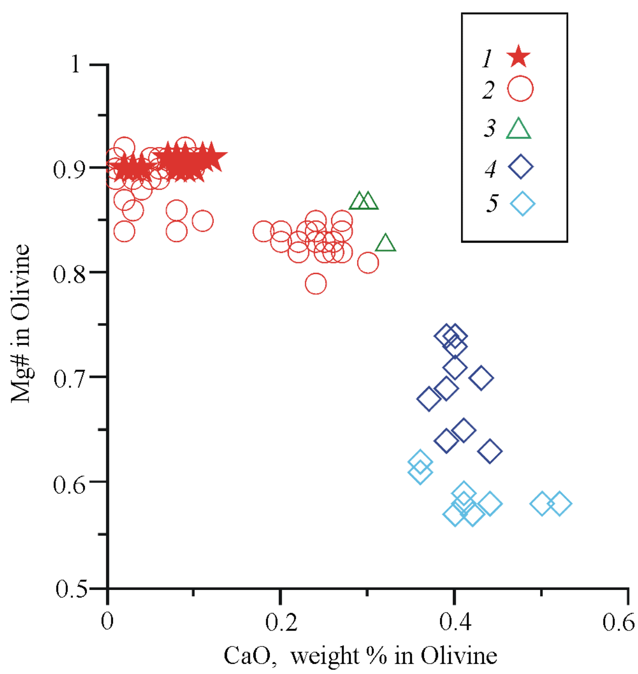

Figure 3. Variations in the CaO content and Mg# of olivine from: 1 – mantle xenoliths of spinel lherzolites, 2 – alkaline olivine basalts from Zhokhov Island, 3 – dolerite xenolith, 4 – magnesian alkaline basalts from Bennett Island, 5 – alkaline basalts from Bennett Island.

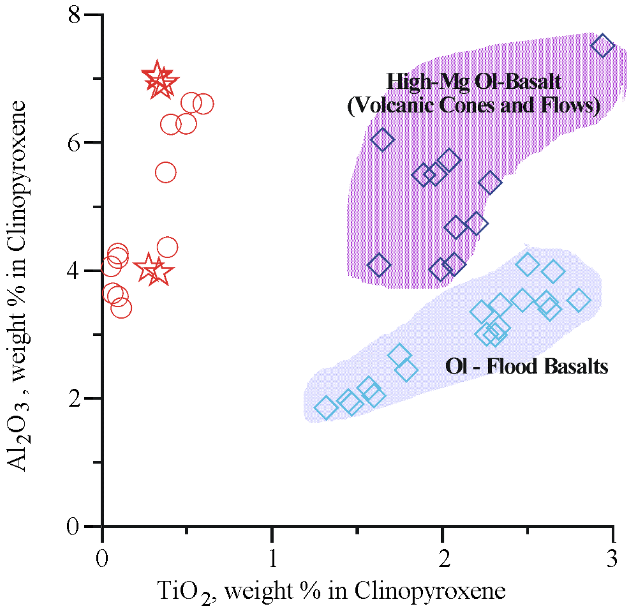

Figure 4. Variations in the Al_2O_3 and TiO_2 contents in clinopyroxene in volcanic rocks and mantle xenoliths from the De Long islands. See Figure 3 for symbol explanations.

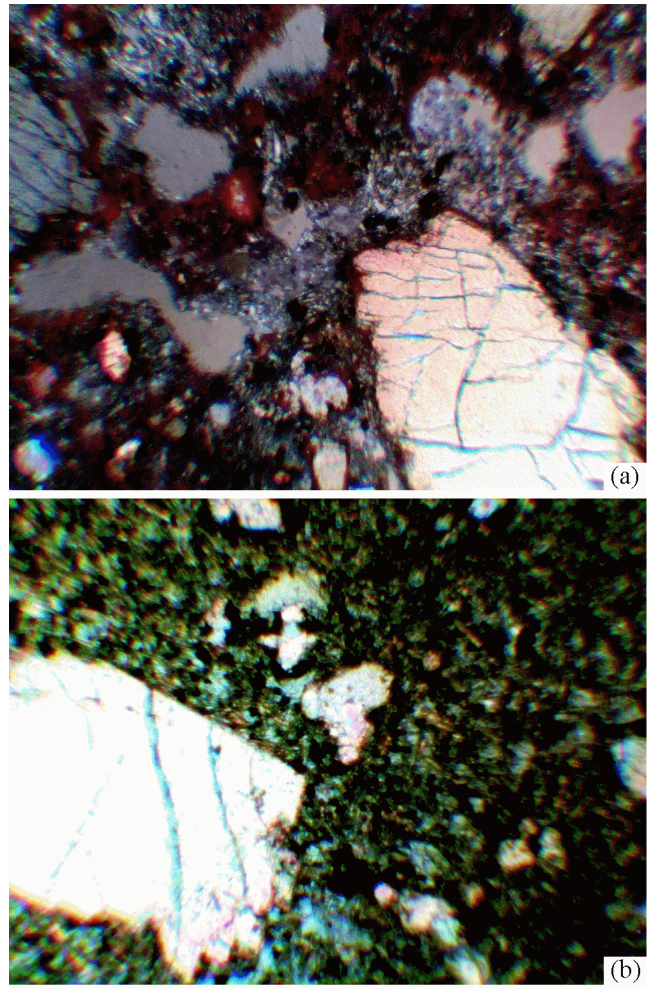

Figure 6. Microphotograph of limburgite (petrographic thin section) from Zhokhov Island, sample DL-32 (a), and from Vil'kitskii Island, sample DL-39 (b). Parallel polarizers, magnification 72×.

The groundmass of these volcanics consists of glass with discernible fluidal structures and submerged rare olivine phenocrysts. All of the aforementioned volcanic rocks are altered very weakly: some olivine phenocrysts are surrounded by thin hematite rinds, caused by oxidation during the eruption of the lava flows. Olivine in the crystalline rocks is partly replaced by bowlingite, and clinopyroxene is sporadically uralitized. The chemistry of the minerals composing basaltoids from Zhokhov Island is discussed below.

As was mentioned above, lava flows on Zhokhov Island contain two xenolith suites: crustal and mantle. The former comprises rare xenoliths found exclusively in the southwestern shore of the island. There a single dolerite sample with a microgabbro texture was taken (Figure 7) from an isolated fragment in a lava flow of porous basalt. This dolerite consisted of olivine, plagioclase, and clinopyroxene and showed evidence of low-temperature metamorphism (Chl + Act) to the greenschist facies. Other xenoliths found nearby consisted of massive, aphanitic, pale green rocks composed almost entirely of carbonate material and volumetrically subordinate chlorite and rare olivine relics. These rocks resembled most closely strongly altered aphyric basalts. In the same exposure where the aforementioned xenoliths were sampled, we found a single round xenolith of typical quartzite with a characteristic mosaic texture (Figure 8).

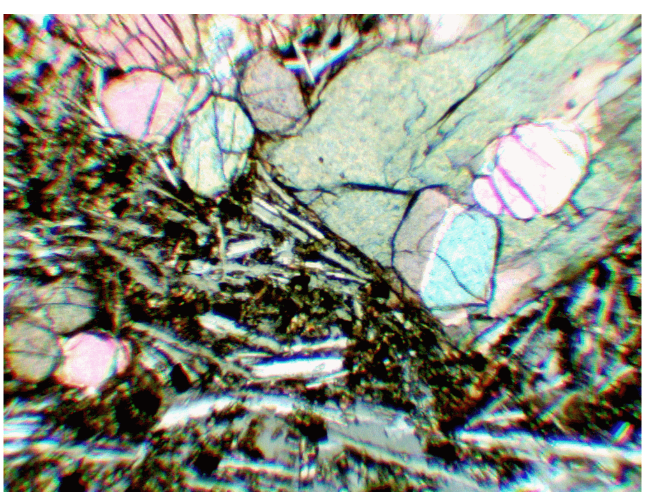

Figure 5. Microphotograph of alkaline olivine basalt (petrographic thin section) from Zhokhov Island, sample DL-1. Crossed polarizers, magnification 72×.

The suite of mantle xenoliths, which were found in all varieties of the volcanic rocks in Zhokhov Island, consisted of spinel lherzolite xenoliths of lens-shaped (flattened) morphology (Figure 9). These rocks consisted of olivine, clino-

Table 1. Mineral chemistry in volcanic and xenolith's suites of magmatic complexes of De Long Islands

Locality	Rock Descripition	SiO_2 Cpx	TiO_2 Cpx	Al_2O_3 Cpx	FeO* Cpx	MnO Cpx	MgO Cpx	CaO Cpx	Na_2O Cpx	Cr_2O_3 Cpx	NiO Cpx	Mg# Cpx
Bennet Is.	Alkaline Basalt	49.96	2.78	3.52	8.97	0.15	11.6	21.91	0.88	0	n.d.	0.69
Bennet Is.	Alkaline Basalt	50.03	2.29	2.98	8.85	0.2	11.94	22.1	0.91	0.04	n.d.	0.3
Bennet Is.	Alkaline Basalt	49.35	2.59	3.49	9.03	0.2	12.07	21.95	0.8	0.03	n.d.	0.7
Bennet Is.	Alkaline Basalt	49.27	2.61	3.38	8.94	0.2	11.93	22.16	0.84	0	n.d.	0.7
Bennet Is.	Alkaline Basalt	51.22	1.58	2.03	7.83	0.18	13.06	22.05	0.45	0.01	n.d.	0.74
Bennet Is.	Alkaline Basalt	51.58	1.55	2.15	7.81	0.21	13.11	22.51	0.5	0	n.d.	0.74
Bennet Is.	Alkaline Basalt	49.82	1.77	2.43	8.47	0.24	12.31	22.19	0.77	0	n.d.	0.72
Bennet Is.	Alkaline Basalt	49.1	2.24	2.99	8.79	0.17	11.96	22.02	0.68	0.01	n.d.	0.7
Bennet Is.	Alkaline Basalt	48.98	2.31	3.09	8.61	0.18	11.74	21.73	0.9	0.03	n.d.	0.7
Bennet Is.	Alkaline Basalt	51.96	1.3	1.84	9.76	0.17	11.61	22.6	1.05	0	n.d.	0.68
Bennet Is.	Alkaline Basalt	49.42	2.32	3.45	9.29	0.15	11.63	20.96	0.93	0	n.d.	0.69
Bennet Is.	Alkaline Basalt	50.99	2.48	4.08	9.41	0.19	11.59	20.38	0.97	0.02	n.d.	0.68
Bennet Is.	Alkaline Basalt	49.14	2.45	3.52	9.09	0.27	12.21	21.35	0.8	0.02	n.d.	0.7
Bennet Is.	Alkaline Basalt	48.45	2.63	3.97	8.88	0.17	12.2	21.1	0.69	0	n.d.	0.7
Bennet Is.	Alkaline Basalt	51.51	1.73	2.66	8.32	0.2	12.94	21.57	0.53	0.05	n.d.	0.73
Bennet Is.	Alkaline Basalt	52.01	1.45	1.9	8.33	0.21	13.35	21.46	0.51	0.03	n.d.	0.74
Bennet Is.	Alkaline Basalt	51.61	1.43	1.95	8.36	0.19	13.36	21.32	0.52	0	n.d.	0.74
Bennet Is.	Alkaline Basalt	49.12	2.21	3.34	8.71	0.2	12.08	21.48	0.68	0.03	n.d.	0.71
Locality	Rock Descripition	SiO_2 Ol	TiO_2 Ol	Al_2O_3 Ol	FeO* Ol	MnO Ol	MgO Ol	CaO Ol	Na_2O Ol	Cr_2O_3 Ol	NiO Ol	Mg# Ol
Bennet Is.	Alkaline Basalt	36.37	n.d.	n.d.	32.92	0.55	29.61	0.36	n.d.	n.d.	n.d.	0.61
Bennet Is.	Alkaline Basalt	36.05	n.d.	n.d.	34.93	0.69	27.53	0.41	n.d.	n.d.	n.d.	0.58
Bennet Is.	Alkaline Basalt	36.14	n.d.	n.d.	32.44	0.57	30.08	0.36	n.d.	n.d.	n.d.	0.62
Bennet Is.	Alkaline Basalt	35.95	n.d.	n.d.	33.82	0.62	28.23	0.41	n.d.	n.d.	n.d.	0.59
Bennet Is.	Alkaline Basalt	36.1	n.d.	n.d.	34.4	0.71	27.33	0.5	n.d.	n.d.	n.d.	0.58
Bennet Is.	Alkaline Basalt	36.28	n.d.	n.d.	34.82	0.67	27.35	0.52	n.d.	n.d.	n.d.	0.58
Bennet Is.	Alkaline Basalt	36.3	n.d.	n.d.	34.68	0.71	27.37	0.44	n.d.	n.d.	n.d.	0.58
Bennet Is.	Alkaline Basalt	36.11	n.d.	n.d.	35.83	0.64	27.04	0.4	n.d.	n.d.	n.d.	0.57
Bennet Is.	Alkaline Basalt	35.9	n.d.	n.d.	35.25	0.75	27.2	0.42	n.d.	n.d.	n.d.	0.57
Locality	Rock Descripition	SiO_2 Cpx	TiO_2 Cpx	Al_2O_3 Cpx	FeO* Cpx	MnO Cpx	MgO Cpx	CaO Cpx	Na_2O Cpx	Cr_2O_3 Cpx	NiO Cpx	Mg# Cpx
Bennet Is.	Mg- Alkaline Basalt	48.95	1.63	6.03	6.38	0.11	13.21	22.37	0.25	0.54	n.d.	0.78
Bennet Is.	Mg- Alkaline Basalt	47.87	2.02	5.71	7.48	0.05	12.21	22.9	0.35	0.21	n.d.	0.74
Bennet Is.	Mg- Alkaline Basalt	47.77	2.26	5.36	7.8	0.11	12.11	22.74	0.51	0.1	n.d.	0.73
Bennet Is.	Mg- Alkaline Basalt	48.76	2.06	4.66	7.66	0.17	12.89	22.28	0.62	0.02	n.d.	0.75
Bennet Is.	Mg- Alkaline Basalt	49.38	2.05	4.08	7.33	0.16	12.49	22.25	0.6	0	n.d.	0.75
Bennet Is.	Mg- Alkaline Basalt	47.97	1.87	5.48	7.15	0.14	12.38	22.51	0.36	0.24	n.d.	0.75
Bennet Is.	Mg- Alkaline Basalt	48.13	1.94	5.49	7.27	0.07	12.36	22.75	0.37	0.19	n.d.	0.75
Bennet Is.	Mg- Alkaline Basalt	45.64	2.92	7.5	8.82	0.15	11.27	22.19	0.88	0.09	n.d.	0.69
Bennet Is.	Mg- Alkaline Basalt	50.56	1.61	4.07	7.72	0.15	13.2	22.23	0.54	0.15	n.d.	0.75
Bennet Is.	Mg- Alkaline Basalt	48.74	2.18	4.72	7.32	0.1	12.56	22.66	0.61	0.04	n.d.	0.75
Bennet Is.	Mg- Alkaline Basalt	49.66	1.97	4	7.15	0.18	12.51	22.48	0.62	0	n.d.	0.75

Table 1. Continued

Locality	Rock Descripition	SiO_2 Ol	TiO_2 Ol	Al_2O_3 Ol	FeO Ol	MnO Ol	MgO Ol	CaO Ol	Na_2O Ol	Cr_2O_3 Ol	NiO Ol	Mg# Ol
Bennet Is.	Mg- Alkaline Basalt	37.56	n.d.	n.d.	27.62	0.52	33.38	0.37	n.d.	n.d.	n.d.	0.68
Bennet Is.	Mg- Alkaline Basalt	37.45	n.d.	n.d.	29.64	0.56	30.66	0.39	n.d.	n.d.	n.d.	0.64
Bennet Is.	Mg- Alkaline Basalt	37.96	n.d.	n.d.	24.87	0.42	35.47	0.4	n.d.	n.d.	n.d.	0.71
Bennet Is.	Mg- Alkaline Basalt	37.77	n.d.	n.d.	26.68	0.5	34.24	0.39	n.d.	n.d.	n.d.	0.69
Bennet Is.	Mg- Alkaline Basalt	37.78	n.d.	n.d.	25.64	0.43	34.19	0.43	n.d.	n.d.	n.d.	0.7
Bennet Is.	Mg- Alkaline Basalt	37.8	n.d.	n.d.	25.45	0.46	35.32	0.43	n.d.	n.d.	n.d.	0.7
Bennet Is.	Mg- Alkaline Basalt	38.38	n.d.	n.d.	23.81	0.47	36.33	0.4	n.d.	n.d.	n.d.	0.73
Bennet Is.	Mg- Alkaline Basalt	37.9	n.d.	n.d.	23.33	0.4	36.89	0.4	n.d.	n.d.	n.d.	0.74
Bennet Is.	Mg- Alkaline Basalt	38.3	n.d.	n.d.	22.92	0.35	37.71	0.39	n.d.	n.d.	n.d.	0.74
Bennet Is.	Mg- Alkaline Basalt	36.84	n.d.	n.d.	30.27	0.53	32.12	0.41	n.d.	n.d.	n.d.	0.65
Bennet Is.	Mg- Alkaline Basalt	36.74	n.d.	n.d.	30.95	0.55	30.71	0.44	n.d.	n.d.	n.d.	0.63
Locality	Rock Descripition	SiO_2 Cpx	TiO_2 Cpx	Al_2O_3 Cpx	FeO* Cpx	MnO Cpx	MgO Cpx	CaO Cpx	Na_2O Cpx	Cr_2O_3 Cpx	NiO Cpx	Mg# Cpx
Zhokhov Is.	Ol-basalts	51.9	0.04	4.05	2.08	0	15.25	20.73	1.88	1.58	0.01	0.93
Zhokhov Is.	Ol-basalts	51.99	0.08	4.18	2.01	0.02	15.24	20.84	1.75	1.31	0.03	0.93
Zhokhov Is.	Ol-basalts	53.1	0.08	4.25	1.95	0.1	14.98	20.68	1.87	1.41	0.03	0.93
Zhokhov Is.	Ol-basalts	50.21	0.58	6.59	3.05	0.05	15.38	18.73	1.61	1.16	0	0.9
Zhokhov Is.	Ol-basalts	51.52	0.51	6.61	3.05	0.04	15.57	18.31	1.72	1.12	0.07	0.9
Zhokhov Is.	Ol-basalts	51.8	0.48	6.28	2.66	0.1	14.65	20.72	1.56	0.62	0.03	0.91
Zhokhov Is.	Ol-basalts	52.96	0.1	3.4	2.49	0.09	17.45	21.44	0.67	0.89	0.04	0.93
Zhokhov Is.	Ol-basalts	51.32	0.08	3.58	2.6	0.08	17.25	21.36	0.57	1.05	0.1	0.92
Zhokhov Is.	Ol-basalts	52.43	0.05	3.63	2.47	0.08	17.25	21.46	0.65	1.05	0	0.93
Zhokhov Is.	Ol-basalts	51.69	0.39	6.27	2.82	0.08	15.85	19.63	1.52	1.01	0.05	0.91
Zhokhov Is.	Ol-basalts	51.83	0.36	5.52	2.64	0.07	14.67	21.6	1.62	0.7	0.06	0.91
Zhokhov Is.	Ol-basalts	50.46	0.37	4.35	2.16	0.04	15.47	21.57	1.48	0.77	0	0.93
Locality	Rock Descripition	SiO_2 Opx	TiO_2 Opx	Al_2O_3 Opx	FeO* Opx	MnO Opx	MgO Opx	CaO Opx	Na_2O Opx	Cr_2O_3 Opx	NiO Opx	Mg# Opx
Zhokhov Is.	Ol-basalts	55.79	0.05	3.81	5.69	0.17	32.66	0.53	0.1	0.37	0.06	0.91
Zhokhov Is.	Ol-basalts	54.42	0.05	3.78	5.78	0.15	32.92	0.57	0.05	0.37	0.1	0.91
Zhokhov Is.	Ol-basalts	53.22	0.01	3.17	5.28	0.11	32.62	0.98	0.04	0.68	0	0.92
Zhokhov Is.	Ol-basalts	54.74	0.05	3.82	5.21	0.24	32.24	1	0.08	0.68	0.06	0.92
Zhokhov Is.	Ol-basalts	54.32	0.17	4.22	5.67	0.12	32.06	1.02	0.26	0.66	0.11	0.91
Zhokhov Is.	Ol-basalts	54.15	0.23	3.89	5.47	0.14	31.77	1.01	0.25	0.71	0.08	0.91
Zhokhov Is.	Ol-basalts	54.76	0.07	3.21	5.66	0.11	33.55	0.44	0.04	0.37	0.11	0.91
Locality	Rock Descripition	SiO_2 Ol	TiO_2 Ol	Al_2O_3 Ol	FeO Ol	MnO Ol	MgO Ol	CaO Ol	Na_2O Ol	Cr_2O_3 Ol	NiO Ol	Mg# Ol
Zhokhov Is.	Ol-basalts	40.91	n.d.	n.d.	8.02	0.11	50.62	0.02	n.d.	0.01	0.38	0.92
Zhokhov Is.	Ol-basalts	39.78	n.d.	n.d.	13.11	0.21	45.43	0.03	n.d.	0.05	0.23	0.86
Zhokhov Is.	Ol-basalts	39.37	n.d.	n.d.	15.27	0.16	42.04	0.6	n.d.	0	0.21	0.83
Zhokhov Is.	Ol-basalts	39.89	n.d.	n.d.	15.01	0.29	43.91	0.02	n.d.	0.02	0.2	0.84
Zhokhov Is.	Ol-basalts	39.94	n.d.	n.d.	15.43	0.2	43.12	0.26	n.d.	0.02	0.38	0.83
Zhokhov Is.	Ol-basalts	38	n.d.	n.d.	17.8	0.24	41.8	0.3	n.d.	0.11	0.22	0.81
Zhokhov Is.	Ol-basalts	38.96	n.d.	n.d.	17.12	0.19	42.95	0.25	n.d.	0.05	0.28	0.82

Table 1. Continued

Locality	Rock Descripition	SiO_2 Ol	TiO_2 Ol	Al_2O_3 Ol	FeO Ol	MnO Ol	MgO Ol	CaO Ol	Na_2O Ol	Cr_2O_3 Ol	NiO Ol	Mg# Ol
Zhokhov Is.	Ol-basalts	38.81	n.d.	n.d.	12.73	0.15	45.43	0.08	n.d.	0.04	0.29	0.86
Zhokhov Is.	Ol-basalts	39.44	n.d.	n.d.	15.85	0.22	42.87	0.2	n.d.	0.01	0.22	0.83
Zhokhov Is.	Ol-basalts	39.42	n.d.	n.d.	14.7	0.12	44.16	0.08	n.d.	0.01	0.27	0.84
Zhokhov Is.	Ol-basalts	39.48	n.d.	n.d.	15	0.18	43.79	0.2	n.d.	0	0.25	0.84
Zhokhov Is.	Ol-basalts	39.76	n.d.	n.d.	9.9	0.12	47.66	0.04	n.d.	0	0.38	0.9
Zhokhov Is.	Ol-basalts	40.2	n.d.	n.d.	9.52	0.18	49.19	0.04	n.d.	0.01	0.35	0.9
Zhokhov Is.	Ol-basalts	39.85	n.d.	n.d.	9.15	0.16	48.02	0.07	n.d.	0.08	0.33	0.9
Zhokhov Is.	Ol-basalts	39.64	n.d.	n.d.	9.12	0.17	49.01	0.08	n.d.	0.02	0.46	0.91
Zhokhov Is.	Ol-basalts	40.38	n.d.	n.d.	9.81	0.17	47.49	0.06	n.d.	0.01	0.36	0.9
Zhokhov Is.	Ol-basalts	40.32	n.d.	n.d.	8.95	0.18	49.39	0.07	n.d.	0.02	0.39	0.91
Zhokhov Is.	Ol-basalts	40.66	n.d.	n.d.	8.67	0.06	48.44	0.08	n.d.	0.03	0.44	0.91
Zhokhov Is.	Ol-basalts	41.27	n.d.	n.d.	8.99	0.2	48.5	0.06	n.d.	0.02	0.44	0.91
Zhokhov Is.	Ol-basalts	39.68	n.d.	n.d.	16.64	0.18	41.84	0.26	n.d.	0.04	0.19	0.82
Zhokhov Is.	Ol-basalts	38.55	n.d.	n.d.	17.03	0.17	42.59	0.27	n.d.	0	0.19	0.82
Zhokhov Is.	Ol-basalts	39.08	n.d.	n.d.	16.83	0.22	41.74	0.22	n.d.	0.03	0.16	0.82
Zhokhov Is.	Ol-basalts	39.84	n.d.	n.d.	9.74	0.13	46.44	0.06	n.d.	0.08	0.32	0.89
Zhokhov Is.	Ol-basalts	38.91	n.d.	n.d.	9.34	0.16	47.65	0.01	n.d.	0	0.36	0.9
Zhokhov Is.	Ol-basalts	40.33	n.d.	n.d.	8.23	0.11	49.78	0.09	n.d.	0.04	0.33	0.92
Zhokhov Is.	Ol-basalts	40.57	n.d.	n.d.	9.15	0.16	48.4	0.02	n.d.	0.01	0.42	0.9
Zhokhov Is.	Ol-basalts	40.46	n.d.	n.d.	9.41	0.11	47.71	0.06	n.d.	0.02	0.37	0.9
Zhokhov Is.	Ol-basalts	39.49	n.d.	n.d.	10	0.11	46.2	0.03	n.d.	0.02	0.38	0.89
Zhokhov Is.	Ol-basalts	40.29	n.d.	n.d.	9.24	0.09	47.41	0.06	n.d.	0.01	0.4	0.9
Zhokhov Is.	Ol-basalts	40.99	n.d.	n.d.	9.51	0.14	48.33	0.1	n.d.	0	0.38	0.9
Zhokhov Is.	Ol-basalts	40.47	n.d.	n.d.	9.47	0.09	49.57	0.08	n.d.	0.41	0.16	0.9
Zhokhov Is.	Ol-basalts	40.83	n.d.	n.d.	9.14	0.13	48.94	0.09	n.d.	0.04	0.42	0.91
Zhokhov Is.	Ol-basalts	40.3	n.d.	n.d.	9.11	0.11	49.38	0.1	n.d.	0.01	0.34	0.91
Zhokhov Is.	Ol-basalts	41.49	n.d.	n.d.	9.03	0.08	47.85	0.08	n.d.	0.07	0.37	0.9
Zhokhov Is.	Ol-basalts	40.9	n.d.	n.d.	9.03	0.07	48.7	0.01	n.d.	0.02	0.35	0.91
Zhokhov Is.	Ol-basalts	40.41	n.d.	n.d.	9.21	0.13	49.21	0.01	n.d.	0.05	0.4	0.91
Zhokhov Is.	Ol-basalts	40.3	n.d.	n.d.	8.56	0.16	48.81	0.06	n.d.	0	0.38	0.91
Zhokhov Is.	Ol-basalts	40.3	n.d.	n.d.	8.56	0.16	48.81	0.06	n.d.	0	0.38	0.91
Zhokhov Is.	Ol-basalts	40.3	n.d.	n.d.	8.56	0.16	48.81	0.06	n.d.	0	0.38	0.91
Zhokhov Is.	Ol-basalts	41.15	n.d.	n.d.	9.8	0.14	47.66	0.01	n.d.	0.04	0.38	0.9
Zhokhov Is.	Ol-basalts	40.93	n.d.	n.d.	9.07	0.11	48.72	0.06	n.d.	0.01	0.31	0.91
Zhokhov Is.	Ol-basalts	40.8	n.d.	n.d.	9.97	0.08	47.59	0.01	n.d.	0.08	0.39	0.89
Zhokhov Is.	Ol-basalts	40.87	n.d.	n.d.	10.18	0.09	47.23	0.05	n.d.	0.04	0.24	0.89
Zhokhov Is.	Ol-basalts	39.41	n.d.	n.d.	10.58	0.12	47.76	0.05	n.d.	0.03	0.4	0.89
Zhokhov Is.	Ol-basalts	41.07	n.d.	n.d.	9.4	0.14	47.74	0.08	n.d.	0.02	0.41	0.9
Zhokhov Is.	Ol-basalts	40.86	n.d.	n.d.	9.64	0.17	48.11	0.07	n.d.	0.06	0.29	0.9
Zhokhov Is.	Ol-basalts	39.71	n.d.	n.d.	11.33	0.16	46.75	0.04	n.d.	0.01	0.38	0.88

Table 1. Continued

Locality	Rock Descripition	SiO_2 Ol	TiO_2 Ol	Al_2O_3 Ol	FeO Ol	MnO Ol	MgO Ol	CaO Ol	Na_2O Ol	Cr_2O_3 Ol	NiO Ol	Mg# Ol
Zhokhov Is.	Ol-basalts	39.58	n.d.	n.d.	15.92	0.23	43.48	0.25	n.d.	0.02	0.25	0.83
Zhokhov Is.	Ol-basalts	40.77	n.d.	n.d.	14.86	0.15	44.64	0.18	n.d.	0.04	0.31	0.84
Zhokhov Is.	Ol-basalts	39.84	n.d.	n.d.	15.98	0.16	43.52	0.24	n.d.	0.08	0.3	0.83
Zhokhov Is.	Ol-basalts	38.98	n.d.	n.d.	18.82	0.21	40.56	0.24	n.d.	0.04	0.34	0.79
Zhokhov Is.	Ol-basalts	40.6	n.d.	n.d.	12.63	0.16	46	0.02	n.d.	0	0.31	0.87
Zhokhov Is.	Ol-basalts	39.93	n.d.	n.d.	15.48	0.21	43.5	0.22	n.d.	0.08	0.23	0.83
Zhokhov Is.	Ol-basalts	39.21	n.d.	n.d.	15.3	0.21	42.66	0.25	n.d.	0	0.29	0.83
Zhokhov Is.	Ol-basalts	39.6	n.d.	n.d.	15.16	0.18	44.74	0.24	n.d.	0.01	0.27	0.84
Zhokhov Is.	Ol-basalts	39.38	n.d.	n.d.	15.97	0.18	43.05	0.25	n.d.	0.08	0.23	0.83
Zhokhov Is.	Ol-basalts	39.18	n.d.	n.d.	15.42	0.18	43.27	0.22	n.d.	0.04	0.22	0.83
Zhokhov Is.	Ol-basalts	38.86	n.d.	n.d.	14.79	0.18	43.02	0.23	n.d.	0.02	0.24	0.84
Zhokhov Is.	Ol-basalts	39.41	n.d.	n.d.	15.71	0.14	42.23	0.24	n.d.	0.03	0.3	0.83
Zhokhov Is.	Ol-basalts	41.07	n.d.	n.d.	9.55	0.11	48.8	0.09	n.d.	0.08	0.34	0.9
Zhokhov Is.	Ol-basalts	40.5	n.d.	n.d.	9.52	0.09	48.84	0.08	n.d.	0	0.36	0.9
Zhokhov Is.	Ol-basalts	41.03	n.d.	n.d.	9.14	0.17	48.76	0.09	n.d.	0	0.35	0.9
Zhokhov Is.	Ol-basalts	40.62	n.d.	n.d.	9.15	0.12	48.94	0.08	n.d.	0	0.29	0.91
Zhokhov Is.	Ol-basalts	40.99	n.d.	n.d.	8.56	0.14	49.36	0.06	n.d.	0	0.36	0.91
Zhokhov Is.	Ol-basalts	40.33	n.d.	n.d.	9.04	0.12	48.3	0.06	n.d.	0.04	0.39	0.91
Zhokhov Is.	Ol-basalts	41.08	n.d.	n.d.	8.09	0.12	48.38	0.05	n.d.	0	0.34	0.91
Zhokhov Is.	Ol-basalts	38.75	n.d.	n.d.	14.79	0.14	43.29	0.27	n.d.	0.03	0.31	0.84
Zhokhov Is.	Ol-basalts	38.37	n.d.	n.d.	14.04	0.19	43.69	0.11	n.d.	0	0.26	0.85
Zhokhov Is.	Ol-basalts	38.86	n.d.	n.d.	14.14	0.18	43.79	0.27	n.d.	0.1	0.1	0.85
Zhokhov Is.	Ol-basalts	39.4	n.d.	n.d.	14.11	0.15	44.84	0.24	n.d.	0.01	0.24	0.85
Zhokhov Is.	Ol-basalts	40.39	n.d.	n.d.	9.2	0.13	49.21	0.11	n.d.	0	0.37	0.91
Zhokhov Is.	Ol-basalts	40.28	n.d.	n.d.	10.8	0.18	46.86	0.06	n.d.	0.02	0.31	0.89
Zhokhov Is.	Ol-basalts	40.87	n.d.	n.d.	8.54	0.08	48.86	0.07	n.d.	0.07	0.36	0.91
Zhokhov Is.	Dolerite	39.85	n.d.	n.d.	11.97	0.23	45.75	0.29	n.d.	0.04	0.34	0.87
Zhokhov Is.	Dolerite	39.49	n.d.	n.d.	15.33	0.2	42.88	0.32	n.d.	0.1	0.28	0.83
Zhokhov Is.	Dolerite	40.45	n.d.	n.d.	11.82	0.16	46.05	0.3	n.d.	0.04	0.32	0.87
Zhokhov Is.	Sp-Lherzolite	41.08	n.d.	n.d.	9.38	0.13	48.55	0.02	n.d.	0	0.34	0.9
Zhokhov Is.	Sp-Lherzolite	40.73	n.d.	n.d.	9.47	0.11	47.81	0.02	n.d.	0.02	0.4	0.9
Zhokhov Is.	Sp-Lherzolite	41.23	n.d.	n.d.	9.34	0.12	48.73	0.03	n.d.	0.04	0.44	0.9
Zhokhov Is.	Sp-Lherzolite	40.27	n.d.	n.d.	9.36	0.08	48.49	0.03	n.d.	0	0.38	0.9
Zhokhov Is.	Sp-Lherzolite	40.27	n.d.	n.d.	9.63	0.09	47.46	0.04	n.d.	0	0.35	0.9
Zhokhov Is.	Sp-Lherzolite	41.5	n.d.	n.d.	9.44	0.13	48.61	0.1	n.d.	0.02	0.4	0.9
Zhokhov Is.	Sp-Lherzolite	41.06	n.d.	n.d.	9.29	0.21	48.84	0.09	n.d.	0.04	0.31	0.9
Zhokhov Is.	Sp-Lherzolite	41.56	n.d.	n.d.	9.36	0.05	49.44	0.08	n.d.	0.07	0.41	0.9
Zhokhov Is.	Sp-Lherzolite	41.6	n.d.	n.d.	9.1	0.14	49.71	0.11	n.d.	0	0.36	0.91
Zhokhov Is.	Sp-Lherzolite	40.99	n.d.	n.d.	9.26	0.16	50.02	0.07	n.d.	0	0.33	0.91
Zhokhov Is.	Sp-Lherzolite	40.74	n.d.	n.d.	9	0.08	48.88	0.09	n.d.	0	0.29	0.91
Zhokhov Is.	Sp-Lherzolite	41.23	n.d.	n.d.	9.07	0.11	49.32	0.07	n.d.	0	0.39	0.91

Table 1. Continued

Locality	Rock Descripition	SiO_2 Cpx	TiO_2 Cpx	Al_2O_3 Cpx	FeO* Cpx	MnO Cpx	MgO Cpx	CaO Cpx	Na_2O Cpx	Cr_2O_3 Cpx	NiO Cpx	Mg# Cpx
Zhokhov Is.	Sp-Lherzolite	41.45	n.d.	n.d.	9.08	0.2	49.7	0.12	n.d.	0	0.4	0.91
Zhokhov Is.	Sp-Lherzolite	41.25	n.d.	n.d.	8.56	0.22	48.8	0.08	n.d.	0	0.34	0.91
Zhokhov Is.	Sp-Lherzolite	40.1	n.d.	n.d.	8.83	0.12	48.57	0.07	n.d.	0	0.38	0.91
Zhokhov Is.	Sp-Lherzolite	39.9	n.d.	n.d.	9.02	0.13	48.84	0.08	n.d.	0	0.3	0.91
Zhokhov Is.	Sp-Lherzolite	56.62	0.26	4.02	2.57	0.09	16.74	21.29	0.66	1.15	0	0.92
Zhokhov Is.	Sp-Lherzolite	53.33	0.32	3.95	2.57	0.03	16.37	21.56	0.75	1.12	0	0.92
Zhokhov Is.	Sp-Lherzolite	52.73	0.31	7.01	2.92	0.09	15.74	18.61	1.93	1.03	0	0.9
Zhokhov Is.	Sp-Lherzolite	52.53	0.35	6.92	3	0.12	15.48	19.09	2.04	0.99	0	0.9
Zhokhov Is.	Sp-Lherzolite	52.58	0.31	7.03	2.97	0.08	15.68	18.61	2.01	0.99	0	0.9
Zhokhov Is.	Sp-Lherzolite	53.32	0.33	6.87	2.99	0.12	15.94	18.95	1.89	1.06	0	0.9
Locality	Rock Descripition	SiO_2 Opx	TiO_2 Opx	Al_2O_3 Opx	FeO* Opx	MnO Opx	MgO Opx	CaO Opx	Na_2O Opx	Cr_2O_3 Opx	NiO Opx	Mg# Opx
Zhokhov Is.	Sp-Lherzolite	55.07	0.11	5.36	6.51	0.15	30.77	0.63	0.12	0.3	0	0.89
Zhokhov Is.	Sp-Lherzolite	53.81	0.09	5.31	6.46	0.2	30.78	0.71	0.16	0.31	0	0.89
Zhokhov Is.	Sp-Lherzolite	56.52	0.11	5.19	6.48	0.13	30.69	0.72	0.09	0.41	0	0.89
Zhokhov Is.	Sp-Lherzolite	52.85	0.19	6.46	5.93	0.15	32.48	0.89	0.2	0.44	0.13	0.91
Zhokhov Is.	Sp-Lherzolite	55.24	0.14	5.88	5.78	0.14	31.8	0.99	0.2	0.58	0	0.91
Zhokhov Is.	Sp-Lherzolite	54.99	0.09	5.82	5.74	0.11	31	1	0.19	0.57	0	0.91
Zhokhov Is.	Sp-Lherzolite	55.52	0.12	5.73	5.86	0.16	31.59	1.02	0.19	0.6	0	0.91
Zhokhov Is.	Sp-Lherzolite	54.76	0.09	5.82	5.8	0.1	31.38	1.01	0.22	0.59	0	0.91
Zhokhov Is.	Sp-Lherzolite	53.48	0.11	5.69	5.87	0.11	31.31	1	0.17	0.6	0	0.9
Zhokhov Is.	Sp-Lherzolite	54.56	0.13	5.67	5.51	0.12	31.43	0.96	0.24	0.65	0	0.91
Zhokhov Is.	Sp-Lherzolite	53.97	0.09	5.72	5.33	0.16	31.25	0.98	0.23	0.65	0	0.91
Zhokhov Is.	Sp-Lherzolite	54.56	0.11	5.74	5.67	0.11	31.2	1.05	0.25	0.54	0	0.91
Locality	Rock Descripition	SiO_2 Sp	TiO_2 Sp	Al_2O_3 Sp	FeO* Sp	MnO Sp	MgO Sp	CaO Sp	Na_2O Sp	Cr_2O_3 Sp	Cr#.Sp	Mg# Sp
Zhokhov Is.	Sp-Lherzolite	0	0.18	52.65	11.09	0.1	20.44	n.d.	n.d.	16.3	0.17	0.79
Zhokhov Is.	Sp-Lherzolite	0.11	0.23	55	10.48	0.16	21.17	0.01	0.06	10.45	0.11	0.83

Note: n.d. - not determined; All iron has been determined as FeO; 0 - element concentration is less than 0.01 wt %.

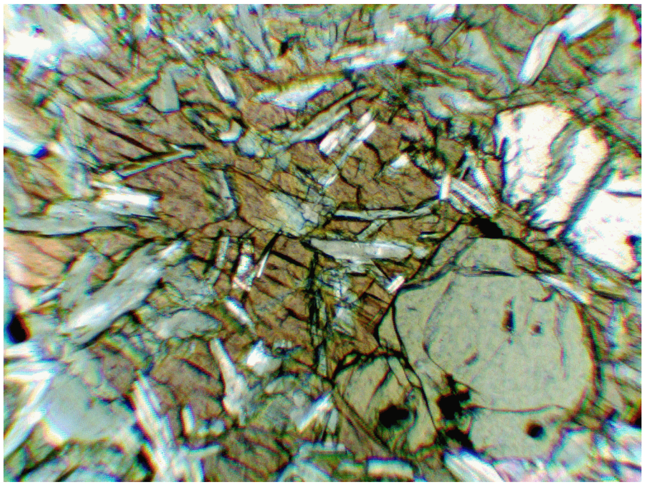

Figure 7. Microphotograph of dolerite (petrographic thin section) from a xenolith, Zhokhov Island, sample DLK-7. Parallel polarizers, magnification 72×.

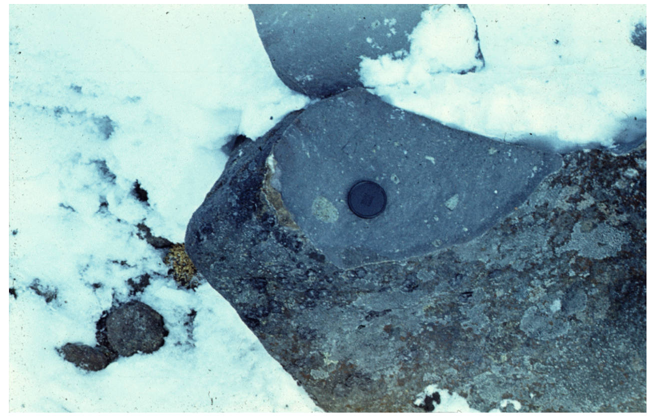

Figure 9. Photograph of spinel lherzolite xenolith in olivine basalt at Zhokhov Island. The magnifying glass (for scale) is 3 cm in diameter.

and orthopyroxene, and spinel and had an idiomorphic-granular texture (Figure 10). The marginal portions of these xenoliths exhibited traces of high-temperature recrystallization, a process manifested in the development of fine-grained secondary olivine.

The central, steepest part of the cliffy exposure in the southern shore of Vil'kitskii Island is made up of massive dark gray volcanics cut by thin shattering zones, in which rocks acquire thin-platy parting. The volcanic pile ubiquitously contains small olivine phenocrysts and spinel lherzolite xenoliths. The volcanic rocks of Vil'kitskii Island are both holocrystalline and predominantly vitreous, with a devitrified matrix. The textures of these rocks and their mineralogy are very close to those of the volcanics described at Devil's Finger Hill on Zhokov Island (Figure 6b). In turn, the mineralogy of xenoliths from Vil'kitskii Island is completely identical to that of mantle xenoliths from Zhokhov Island.

Olivine is the most common mineral in magmatic rocks of the De Long Islands. According to its composition, this olivine was classified into the following groups: (1) Olivine in spinel lherzolite xenoliths, which has a high Mg#, low CaO content, and high NiO. Analogous characteristics are typical of olivine xenocrysts from volcanic rocks of Zhokhov and Vil'kitskii islands. As can be seen in Figure 3, the alkaline basaltoids of Bennett Island contain no xenocryst olivine. (2) Olivine phenocrysts contained in subordinate amounts in lava flows on Zhokhov and Vil'kitskii islands and occurring as major minerals in the basaltoids of Bennett Island. They are high in CaO, have a moderate Mg#, and are low in NiO. This group also includes olivine from the dolerite xenolith found on Zhokhov Island. The maximum CaO and minimum MgO contents are typical of olivine from basaltoids in Bennett Island. Within this compositional field, olivine from

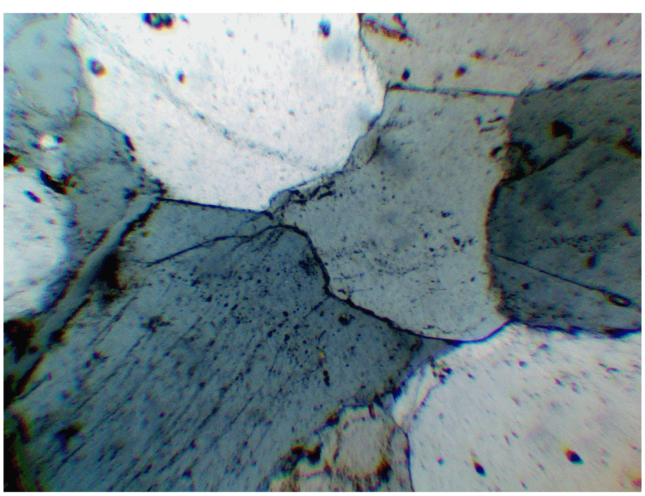

Figure 8. Microphotograph of quartzite (petrographic thin section) from a xenolith, Zhokhov Island, sample DLK-8. Crossed polarizers, magnification 72×.

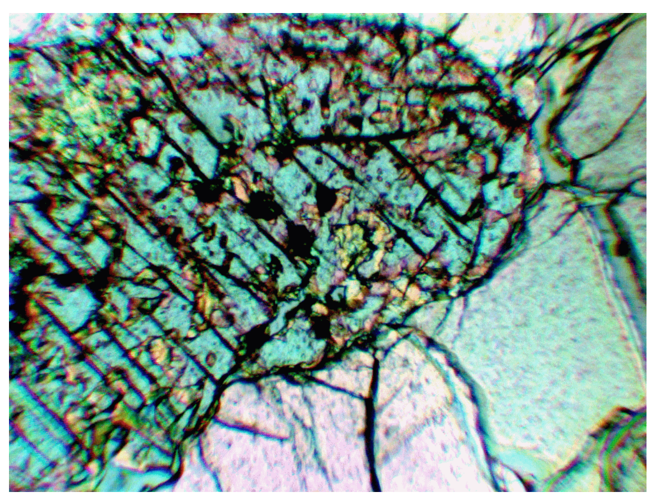

Figure 10. Microphotograph of spinel lherzolite (petrographic thin section) from a xenolith, Zhokhov Island, sample DLK-1. Crossed polarizers, magnification 72×.

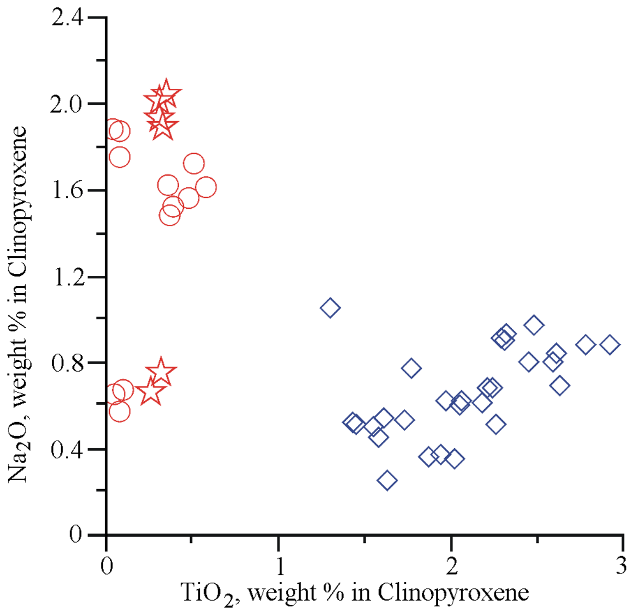

Figure 11. Variations in the Na_2O and TiO_2 contents in clinopyroxene of volcanic rocks and mantle xenoliths from the De Long Islands. See Figure 3 for symbol explanations.

the magnesian silica-undersaturated alkaline basalts is more magnesian than this mineral from the alkaline (according to the systematics in [*Fedorov et al.,* 2002]) basalts. (3) Some olivine phenocrysts in the lava complex of Zhokhov Island have compositions intermediate between those of the olivines of the two aforementioned groups (Figure 3). Obviously, these intermediate compositions were caused by the recrystallization of the mantle material during its interaction with the magmatic melt.

A noteworthy feature of clinopyroxene in the spinel lherzolite xenoliths is its bimodal composition, which is clearly pronounced in the occurrence of two populations: (1) clinopyroxene with high Al_2O_3 and Na_2O contents and relatively low CaO and Cr_2O_3 concenrtations and (2) this mineral with low Al_2O_3 and Na_2O and relatively high CaO and Cr_2O_3 concentrations (Figures 4, 11). Judging from the variations in the indicator parameters, such as (Al + Cr − 2Ti) and (Na + K), clinopyroxene in mantle xenoliths and phenocrysts in volcanic rocks of Zhokhov Island plots within the fields of pyroxene in mantle spinel lherzolite xenoliths and, partly, megacrysts in alkaline basalts [*Aoki,* 1984]. The Ti and Na concentrations in clinopyroxene from the mantle xenoliths of the De Long Islands are close to these values in clinopyroxene from typical spinel lherzolites in continental areas, such as the Ronda Massif, Massif Central, Balmuccia in the Alps, Dreiser-Weier in Germany, and the Ross Sea in Antarctica. As can be seen in the diagrams, clinopyroxene in the alkaline basalts of Bennett island is more magnesian and remarkably more titaniferous than in volcanics on Zhokov and Vil'kitskii islands. It is pertinent to mention that pyroxene from the magnesian silica-undersaturated alkaline basalts of Bennett Island (see above) is higher in Al_2O_3 and lower in Na_2O than the same mineral from the related alkaline basalts. In contrast to pyroxene from volcanic rocks on Zhokhov and Vil'kitskii islands, this pyroxene exhibits a negative correlation between its Mg# and the Na_2O and Al_2O_3 contents, a feature most probably reflecting the fractional crystallization trend of the parental melt.

As the clinopyroxene, orthopyroxene phenocrysts in the lava complex and mantle xenoliths belong to two compositional groups with different Al_2O_3 contents: (1) 3.17–3.54 wt % and (2) 5.19–6.46 wt %. The high-Al compositions are also characterized by higher Na_2O contents (Table 1).

Inasmuch as clinopyroxene phenocrysts in alkaline basalts typically have high Ti contents, there are good grounds to believe that the lavas of Zhokhov and Vil'kitskii islands contain only xenogenic clinopyroxene. Conversely, this mineral occurs in the basaltoids of Bennett Island exclusively as phenocrysts. Since orthopyroxene is atypical of the phenocryst assemblages of alkaline basalts and strongly undersaturated volcanic rocks [*Coombs and Wilkinson,* 1969], this phase in volcanic rocks from the central part of the De Long Islands can be attributed, along with the low-Ti clinopyroxene, to the xenocryst assemblage. It is worth mentioning that the alkaline basaltoids of Bennett Island contain no orthopyroxene at all. The fact that the spinel lherzolite xenoliths contain pyroxene of two populations having significantly different compositions suggests that there could be high-temperature interaction between the xenoliths and the melt entraining them.

Spinel in mantle xenoliths from the central part of the De Long Islands has compositional parameters (Table 1) characteristic of spinel from undepleted mantle peridotites or these rocks without traces of significant melting. A convincing

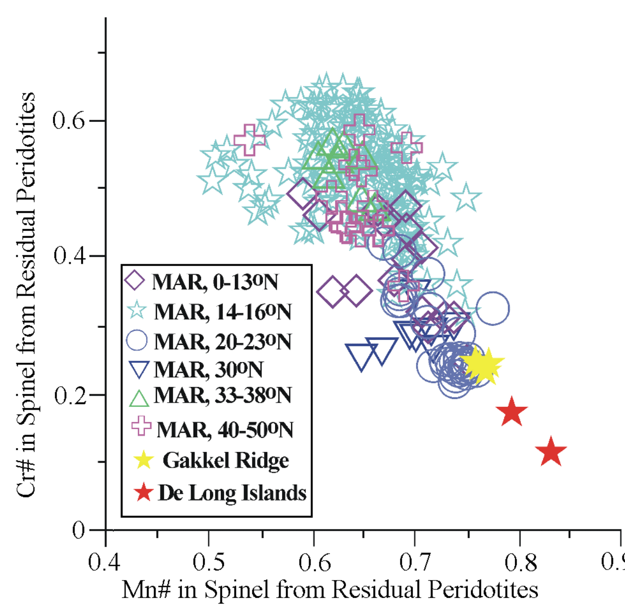

Figure 12. Comparison of the Cr# and Mg# of spinel from spinel lherzolites of Zhokhov Island and this mineral from mantle xenoliths of the Mid-Atlantic Ridge (plume and spreading segments) and the Gakkel Ridge (after [*Hellebrand et al.,* 2002]).

argument in support of this is provided by the comparison of the composition of spinel from mantle xenoliths of Zhokov Island with the composition of this mineral in residual peridotites from the MAR and Gakkel Ridge (Figure 12). As is obvious from the comparison of olivine and spinel compositions in mantle xenoliths from the MAR residual peridotites and mantle xenoliths from the De Long Islands, the degree of depletion of these xenoliths is the closest to this parameter of the least depleted spinel peridotites from MAR (MARK area at 20°–23°N).

The data presented above on the composition of rock-forming minerals in volcanic rocks and xenoliths from Zhokhov and Vil'kitskii islands provide evidence that olivine phenocrysts in the lava complex of these islands is of predominantly xenogenic (mantle) nature, whereas all pyroxene phenocrysts are xenogenic. At the same time, the mantle xenoliths contain both phases of undoubtedly mantle provenance and the assemblage of olivine and pyroxenes produced during the partial recrystallization of these xenoliths during their interaction with the melt. It is also reasonable to hypothesize that the basaltoids of Bennett Island provide no mineralogical indications that mantle material was entrapped by the parental melts.

Available data make it possible to evaluate the temperatures and pressure of the stability of the spinel lherzolites and xenocryst assemblage in volcanic rocks from the central part of the De Long Islands. For this purpose we used the compositions of coexisting clino- and orthopyroxene, olivine and clinopyroxene, and olivine and spinel. The pyroxene geothermometer making use of covariations in the Ca concentration and Mg# in pyroxene [*Lindsley and Anderson,* 1983] enables, according to [*Vaganov and Sokolov,* 1988], reliable temperature evaluations only for low and mildly aluminous compositions. More realistic estimates can be obtained by the two-pyroxene geothermobarometer [*Mercier,* 1980], which was proposed for pyroxenes with broadly varying Al# from lherzolites of the spinel depth facies. This method also allows for pressure evaluating, although, strictly speaking, these estimates are not completely independent, inasmuch as all the calculations are conducted with the same parameters from which the temperature is calculated. The $P-T$ parameters calculated, according to [*Mercier,* 1980], for the crystallization of mantle xenoliths from Zhokhov Island are $T = 1120°$–$970°$C, $P = 25$–12.5 kbar. The olivine–clinopyroxene geothermometer [*Mori and Green,* 1978] enabled us to estimate the maximum crystallization temperature of the olivine–clinopyroxene assemblage in the mantle xenoliths, which was 1211°C. In addition to the geothermometers mentioned above, we also evaluated the temperatures by the orthopyroxene geothermometer [*Sachtleben and Seck,* 1981], olivine–spinel geothermometer [*O'Neil and Wall,* 1987], and the two-pyroxene geothermometer [*Wells,* 1977].

The $P-T$ parameters calculated by the geothermometers and geobarometers listed above demonstrate that there were three major temperature ranges in which the equilibrium phase assemblages of the mantle xenoliths were formed: ~1100°–1200°C, ~1000°C, and ~760–810°C. The lowest temperatures were obtained by the olivine–spinel geothermometer, because the Ca–Mg exchange between pyroxenes

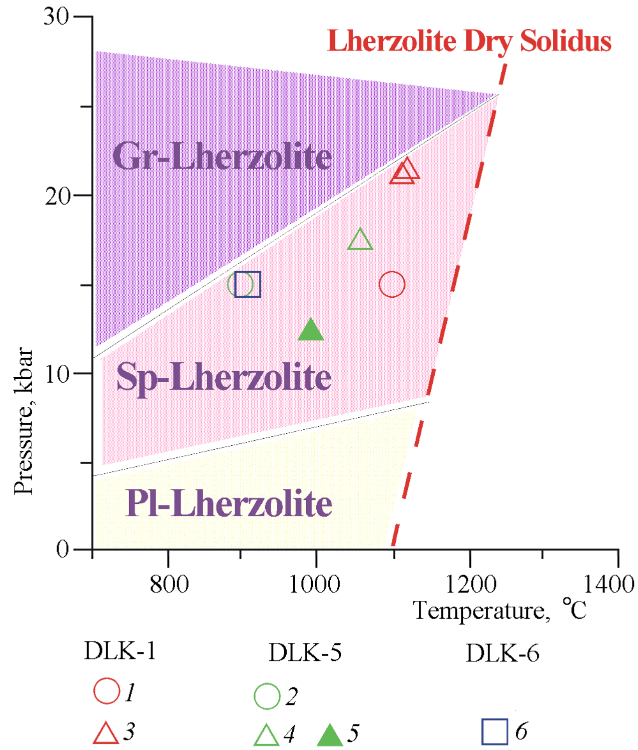

Figure 13. $P-T$ conditions of the crystallization of phase assemblages in spinel lherzolite mantle xenoliths from Zhokhov Island. 1, 2 – Opx [*Lindsley,* 1983]; 3, 4 – Opx [*Mercier,* 1980]; 5 – Cpx [*Mercier,* 1980]; 6 – Ol-Sp [*O'neil, Wall,* 1987].

in spinel peridotites is blocked at higher temperatures than those at which Fe–Mg exchange between olivine and spinel stops. Thus, for spinel lherzolite xenoliths from the De Long Islands, the olivine–spinel geothermometer yielded temperature values corresponding to the latest exhumation stages of the mantle material.

The data presented above clearly delineate the possible $P-T$ trajectory corresponding to the ascent of the magmatic melt in which fragments of mantle rocks (xenoliths) were entrapped at different depth levels (Figure 13). These depths likely corresponded to the following upper mantle levels beneath Zhokhov and Vil'kitskii islands: (1) ~60 km (~21 kbar), (2) ~ 50 km (~16 kbar), and (3) ~45 km (~15 kbar).

Geochemistry of Magmatic Complexes in Bennett, Zhokhov, and Vil'kitskii Islands

The mineralogical characteristics of basaltoids from the lava complexes of Zhokhov, Vil'kitskii, and Bennett islands imply that these are undersaturated alkaline rocks, which is also manifested in the variations in the alkalinity and silicity of these rocks (Table 2, Figure 14). The olivine-phyric basalts from Zhokhov Island define a compositional

Table 2. Major element contents in rocks from magmatic cpmplexes of De Long Islands

Samples	Locality	Rock Descripition	SiO_2	TiO_2	Al_2O_3	FeO^*	MnO	MgO	CaO	Na_2O	K_2O	Cr_2O_3	P_2O_5	LOI	TOTAL
5-83	Bennet Is.	Alkaline Basalt	46.93	1.97	17.67	12.81	0.21	3.12	6.4	3.92	1.29	n.d.	0.72	2.4	98.29
BF-833	Bennet Is.	Mg-Alkaline Basalt	44.3	2.5	14.58	1.11	0.18	8.67	8.76	2.62	0.73	n.d.	0.31	5.65	100.14
BF-834	Bennet Is.	Mg-Alkaline Basalt	44.68	1.51	14.78	10.94	0.19	10.67	9.9	2.45	0.84	n.d.	0.43	1.7	98.41
BF-835	Bennet Is.	Mg-Alkaline Basalt	44.42	1.51	14.83	11.03	0.19	10.39	9.75	2.6	0.84	n.d.	0.45	3.39	99.75
DL-1	Zhokhov Is.	Ol-basalts	48.25	1.98	13.33	10.78	0.16	11.73	8.3	3.28	1.87	0.04	0.46	0.67	100.89
DL-2	Zhokhov Is.	Ol-basalts	48.12	1.98	13.63	10.44	0.16	11.78	8.29	3.23	1.94	0.03	0.48	0.59	100.68
DL-3	Zhokhov Is.	Ol-basalts	47.9	1.97	13.41	10.17	0.16	11.1	8.28	3.54	1.85	0.04	0.5	0.83	99.76
DL-4	Zhokhov Is.	Ol-basalts	47.49	1.9	12.7	10.71	0.18	12.87	7.97	3.62	1.49	0.04	0.45	1.3	100.73
DL-5	Zhokhov Is.	Ol-basalts	45.43	1.9	11.11	9.44	0.17	17.32	6.58	3.5	2.06	0.06	0.76	1.37	100.22
DL-6	Zhokhov Is.	Ol-basalts	46.13	1.86	12.68	10.92	0.18	13.97	7.35	3.57	1.51	0.05	0.52	0.72	99.48
DL-9	Zhokhov Is.	Ol-basalts	49.37	1.83	14.82	10.05	0.16	8.81	8.03	3.53	1.66	0.02	0.47	0.86	99.63
DL-10	Zhokhov Is.	Ol-basalts	46.8	1.83	12.93	11.09	0.18	13.44	7.37	3.53	1.65	0.04	0.54	1.03	100.45
DL-11	Zhokhov Is.	Ol-basalts	46.26	1.74	11.38	11.24	0.18	17.39	6.61	2.89	1.44	0.05	0.47	0.88	100.55
DL-12	Zhokhov Is.	Ol-basalts	46.45	1.83	12.66	11.05	0.18	14.11	7.41	3.27	1.46	0.05	0.52	0.47	99.47
DL-16	Zhokhov Is.	Ol-basalts	47.29	1.88	13.2	11.39	0.18	13.59	7.65	3.69	1.49	0.04	0.52	0.48	101.42
DL-17	Zhokhov Is.	Ol-basalts	47.39	1.89	13.39	11.13	0.18	12.18	7.79	3.45	1.54	0.04	0.52	0.69	100.2
DL-18	Zhokhov Is.	Ol-basalts	46.48	1.94	13.01	11.02	0.18	13.2	7.5	3.76	1.78	0.04	0.63	0.58	100.34
DL-19	Zhokhov Is.	Ol-basalts	50.4	2.08	14.57	10.57	0.16	8.94	7.89	3.83	1.67	0.02	0.49	0.45	101.08
Dl-20a	Zhokhov Is.	Ol-basalts	48.14	2.25	14.11	10.52	0.17	9.48	8.41	3.79	2	0.04	0.57	1.15	100.64
DL-21	Zhokhov Is.	Ol-basalts	48.72	1.9	14.89	10.15	0.17	9.89	7.99	3.5	1.71	0.03	0.48	0.65	100.09
DL-22	Zhokhov Is.	Ol-basalts	50.75	1.91	15.25	10.28	0.16	8.34	8.04	3.88	1.65	0.03	0.48	0.88	101.66
DL-23	Zhokhov Is.	Ol-basalts	45.75	1.9	11.6	10.04	0.18	17.26	6.68	3.72	1.8	0.07	0.58	0.57	100.18
DL-24	Zhokhov Is.	Ol-basalts	45.82	1.85	11.61	9.84	0.16	17.26	6.58	3.59	1.7	0.08	0.61	1.01	100.14
DL-25	Zhokhov Is.	Ol-basalts	45.39	1.92	11.54	9.94	0.16	16.58	6.91	3.54	1.68	0.07	0.62	0.98	99.37
DL-26	Zhokhov Is.	Ol-basalts	45.39	2.15	13.66	9.89	0.17	11.19	7.9	4.75	2.01	0.04	0.7	2.53	100.74
DL-27	Zhokhov Is.	Ol-basalts	47.79	2.02	13.63	10.39	0.16	11.35	8.13	3.66	1.92	0.04	0.5	1.43	101.03
DL-28	Zhokhov Is.	Ol-basalts	44.83	1.46	10.27	11.01	0.18	20.93	5.91	2.48	1.24	0.09	0.46	0.84	99.75
DL-36	Zhokhov Is.	Ol-basalts	48	2.15	14.6	10.3	0.14	9.4	8.4	3	2.2	0.03	0.53	0.15	98.9
DL-13	Zhokhov Is.	Limburgite	42.69	3.13	12.82	10.72	0.16	11.03	8.94	5.3	2.91	0.03	0.97	0.98	99.7
DL-14	Zhokhov Is.	Limburgite	43.47	2.96	12.42	10.57	0.16	12.5	8.67	4.9	2.81	0.04	0.93	0.94	100.39
DL-15	Zhokhov Is.	Limburgite	43.58	2.77	11.99	10.37	0.16	13	8.41	4.85	2.57	0.04	1.02	0.71	99.49
DL-32a	Zhokhov Is.	Limburgite	41.7	2.98	12.1	11.7	0.15	12.5	8.6	4.4	3.2	0.04	0.91	0.6	98.88
DL-33	Zhokhov Is.	Limburgite	42.9	2.79	12.2	11.2	0.15	12.6	8.5	3.9	3	0.06	0.88	0.6	98.78
DL-34	Zhokhov Is.	Limburgite	42.6	2.71	11.6	11.3	0.15	14.1	8.2	4	2.8	0.06	0.98	0.5	99
DL-35	Zhokhov Is.	Limburgite	42.4	2.92	12.3	11.6	0.15	12.3	8.6	4.2	3.2	0.05	0.93	0.65	99.3
DLk-7	Zhokhov Is.	Dolerite	46.02	1.04	12.98	10.74	0.2	17.05	8.63	1.39	0.49	0.13	0.16	2.4	100.56
DLK-1	Zhokhov Is.	Sp-Lherzolite	42.8	0.07	1.2	8.4	0.12	44.4	1.4	n.d.	0.1	0.2	0.03	n.d.	98.72
DLK-2	Zhokhov Is.	Sp-Lherzolite	43.9	0.16	3.2	8.1	0.13	40.3	2.7	n.d.	0.1	0.37	0.04	n.d.	99
DLK-4	Zhokhov Is.	Sp-Lherzolite	43.1	0.13	2.7	7.8	0.13	41.6	2.7	n.d.	n.d.	0.33	0.03	n.d.	98.52
DLK-5	Zhokhov Is.	Sp-Lherzolite	45.57	0.16	2.66	7.87	0.15	40.38	1.38	0.32	0.3	0.71	0.09	0.08	99.92

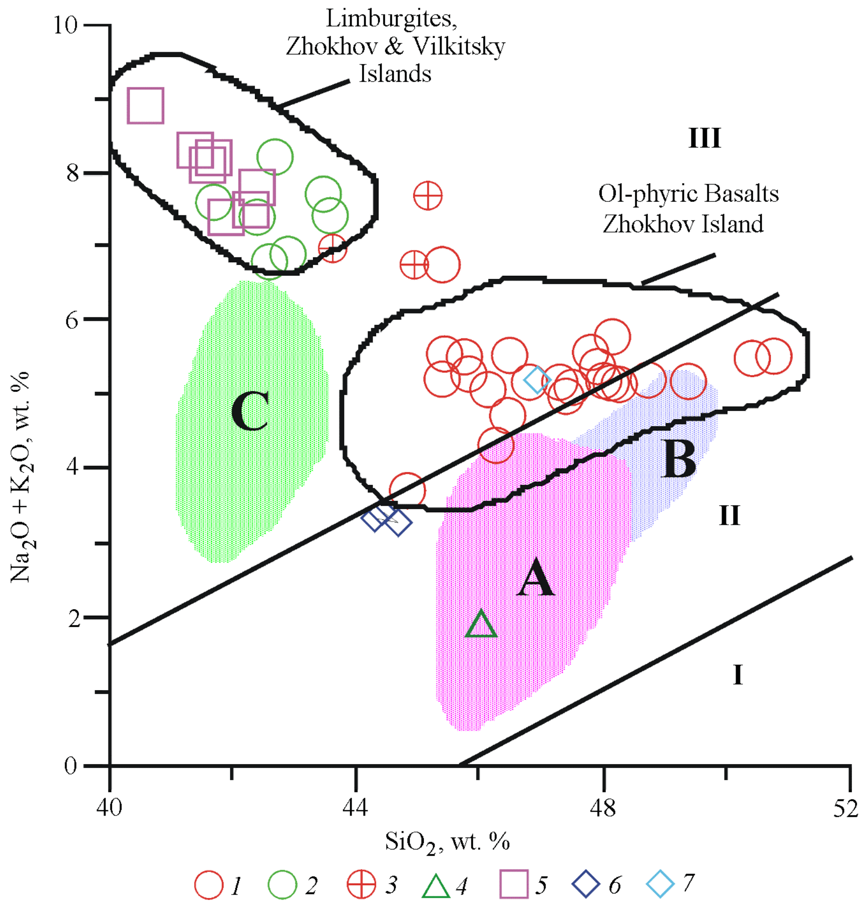

Figure 14. Variations in the alkalinity and silicity of volcanic rocks from the Zhokhov, Vil'kitskii, and Bennett islands. Fields: I – subalkaline rocks, II – mildly high-alkaline and alkaline rocks, III – highly alkaline rocks (after [*Saggerson and Williams,* 1964]); A – alkaline olivine basalts, B – hawaiites, C – olivine nephelinites (after [*Wass,* 1988]). Zhokhov Island: 1 – olivine-phyric basalts, 2 – limburgites, 3 – olivine-phyric basalts (after [*Grachev,* 1999]), 4 – dolerite xenolith. Vil'kitskii Island: 5 – limburgites. Bennett Island: 6 – magnesian silica-undersaturated alkaline basalts, 7 – alkaline basalts (in compliance wit the systematics in [*Fedorov et al.,* 2002]).

field between highly and mildly alkaline rocks (according to the systematics [*Saggerson and Williams,* 1964]) and corresponding to hawaiites. The two discrete group of the Bennett basaltoids (magnesian silica-undersaturated alkaline and alkaline, according to the systematics [*Fedorov et al.,* 2002]; Figure 14 (6 and 7)) distinguished in [*Fedorov et al.,* 2002] fall within the same compositional field in terms of silicity and alkalinity. The second group of compositions, which includes some volcanic rocks from Zhokhov Island (rocks of Devil's Finger Hill) and all volcanics from Vil'kitskii Island, is strongly undersaturated in silica and has alkalinity higher than that of nepheline syenites. These rocks were classified [*Silantyev et al.,* 1991] with limburgite, which are, according to the currently adopted petrographic nomenclature, alkaline volcanic rocks with olivine and clinopyroxene phenocrysts in an alkali-enriched glassy matrix (see above). In the modern TAS classification of volcanic rocks [*Classification...,* 1989], the term "limburgite" is synonymic with glassy basanite. Figure 14 also demonstrates the compositions of some volcanics from Zhokhov Island compiled from [*Grachev,* 1999]. These three compositions plot in the SiO_2–Na_2O + K_2O diagram between the fields of limburgites and olivine alkaline basalts of Zhokhov Island. The dolerite xenolith has these parameters basically different from those of the limburgites and olivine basalts: this rock has a moderate SiO_2 content and relatively low total alkalinity.

The three aforementioned rock groups are characterized by different (Na_2O + K_2O)/Al_2O_3 ratios (agpaitic coefficient). In diagrams based on this parameter, the composition of alkaline basalt from Bennett Island plots not far from the field of alkaline olivine basalts from Zhokhov Island, whereas the compositions of magnesian alkaline basalts form Bennett Island cluster in the vicinity of the composition point of the dolerite xenolith from the lava complex of Zhokhov Island (Figure 15), The (Na_2O + K_2O)/Al_2O_3

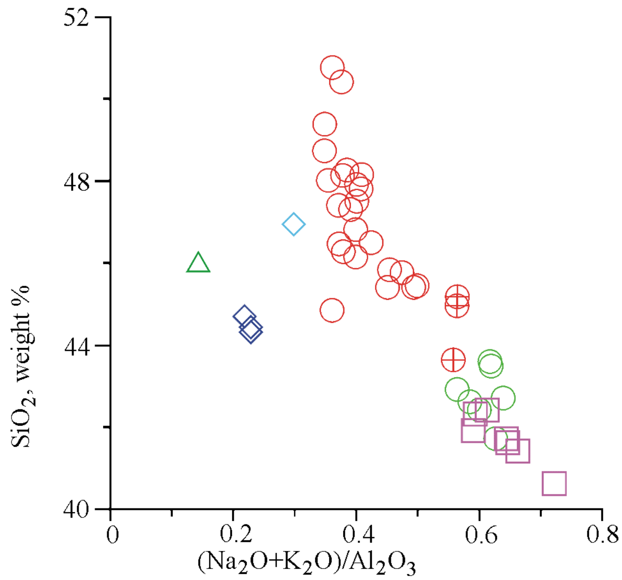

Figure 15. Variations in the SiO_2 content and the $(Na_2O + K_2O)/Al_2O_3$ ratio (agpaitic coefficient) in volcanic rocks from the De Long Islands. See Figures 3 and 14 for symbol explanations.

ratio of the xenogenic dolerite is, in turn, remarkably different from that of the main compositional groups of the volcanics of the De Long Islands, among which the highest sum of alkalis is characteristic of the limburgite from Vil'kitskii Island. The rocks of the limburgite group are characterized by higher P contents than in the alkaline olivine basalts (Figure 16), with the high-Mg volcanic rocks from Bennett Island having P and K contents intermediate between those in the dolerite xenolith and the alkaline olivine basalts from Zhokhov Island.

The contents of major elements in the rocks generally testify that the De Long Islands are composed of two volcanic associations. One of them, which is predominant in the lava complex of Zhokhov Island, is characterized by fractionation trends typical of the picrite–alkali basalt series of within-plate magmatism (Figures 17a, 17b). The rocks of the other association, which compose Vil'kitskii Island and were found in the central part of Zhokhov Island, show no traces of any significant fractionation and are, perhaps, the most primitive volcanic derivatives at the De Long Islands. The high-Mg olivine alkaline basalts and alkaline basalts on Bennett Island can be regarded as the most aluminous members of an evolutionary trend that also includes the basalts from Zhokhov Island (Figure 17b). At the same time, the volcanics from Bennett Island are poorer in SiO_2 and Al_2O_3 (at similar Mg#) than the basalts of Zhokhov Island.

In the context of the problem discussed in this publication, it seems to be expedient to compare the compositions of basaltoids from the De Long Islands and the basalts dredged from the axial zone of the Gakkel Ridge during the AMORE expedition in 2001. Figures 17a and 17b demonstrate that the Mg# and the SiO_2, Al_2O_3, and Na_2O contents of basalts from the Gakkel Ridge are close to these parameters of fractionated volcanic rocks from Zhokhov and Bennett islands. The most enriched basalts of the Gakkel Ridge (which occur exclusively in the western volcanic zone, WVZ, between 7°W and 3°E) also have high Ti#, which is comparable with that of limburgites from Zhokhov and Vil'kitskii islands. At the same time, all basalt analyses from the Gakkel Ridge published in [*Michael et al.,* 2003] have much lower Sr contents (174–274 ppm) than those of the alkaline olivine basalts (340–900 ppm) and limburgites (1190–1410 ppm; Table 3, Figure 18a). The Ti, Sr, and Ba contents in basalts from the Gakkel Ridge (Figure 18b) are close to those in the dolerite xenolith from Zhokhov Island. It is worth noting that these similarities are particularly conspicuous in the basalts sampled at the eastern volcanic zone of the Gakkel Ridge (EVZ, 29°–85°E; Figure 18a). In comparing the geochemistry of magmatic products from the De Long Islands and Gakkel Ridge, it should be taken into account that the data reported in [*Michael et al.,* 2003] led the authors of this publication to suggest that the basalts of the Gakkel Ridge (particularly in the segments between 10°and 40°E, SMZ, a zone of dispersed magmatic activity) are enriched generally more significantly in incompatible elements than average MORB (for example, that from EPR).

It has been demonstrated above that a discriminant geochemical parameter that allows an efficient subdivision of magmatic rocks from Zhokhov, Vil'kitskii, and Bennett islands into three major groups (olivine alkaline basalts, limburgites, and dolerites of the xenolith suite) is the $(Na_2O + K_2O)/Al_2O_3$ ratio. Comparing the variations of this ratio in the rocks with the $(La/Sm)_{cn}$ ratio, conventionally used as an indicator of the degree of enrichment, it can be readily seen (Figure 19a) that the limburgites are enriched

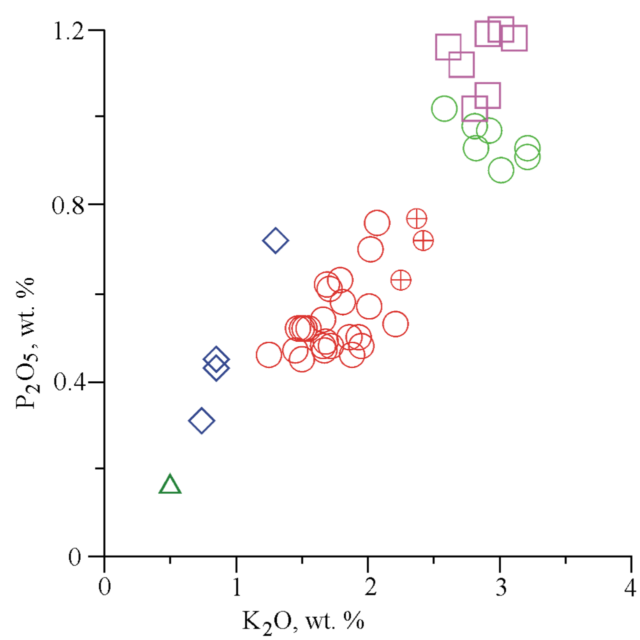

Figure 16. Variations in the K_2O and P_2O_5 contents in volcanic rocks from the De Long Islands. See Figures 3 and 14 for symbol explanations.

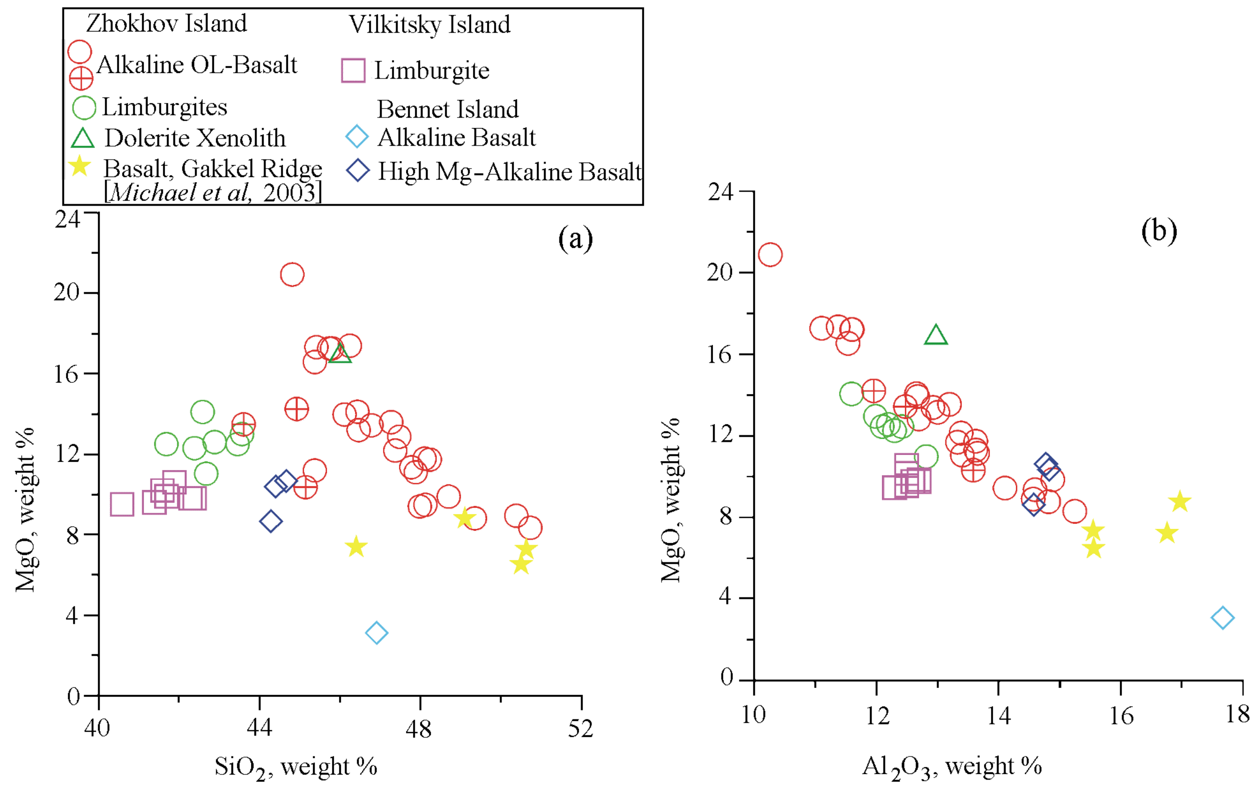

Figure 17. Fractionation trends for basaltoids at the De Long Islands: (a) SiO_2–MgO and (b) Al_2O_3–MgO diagrams. See Figures 3 and 14 for symbol explanations.

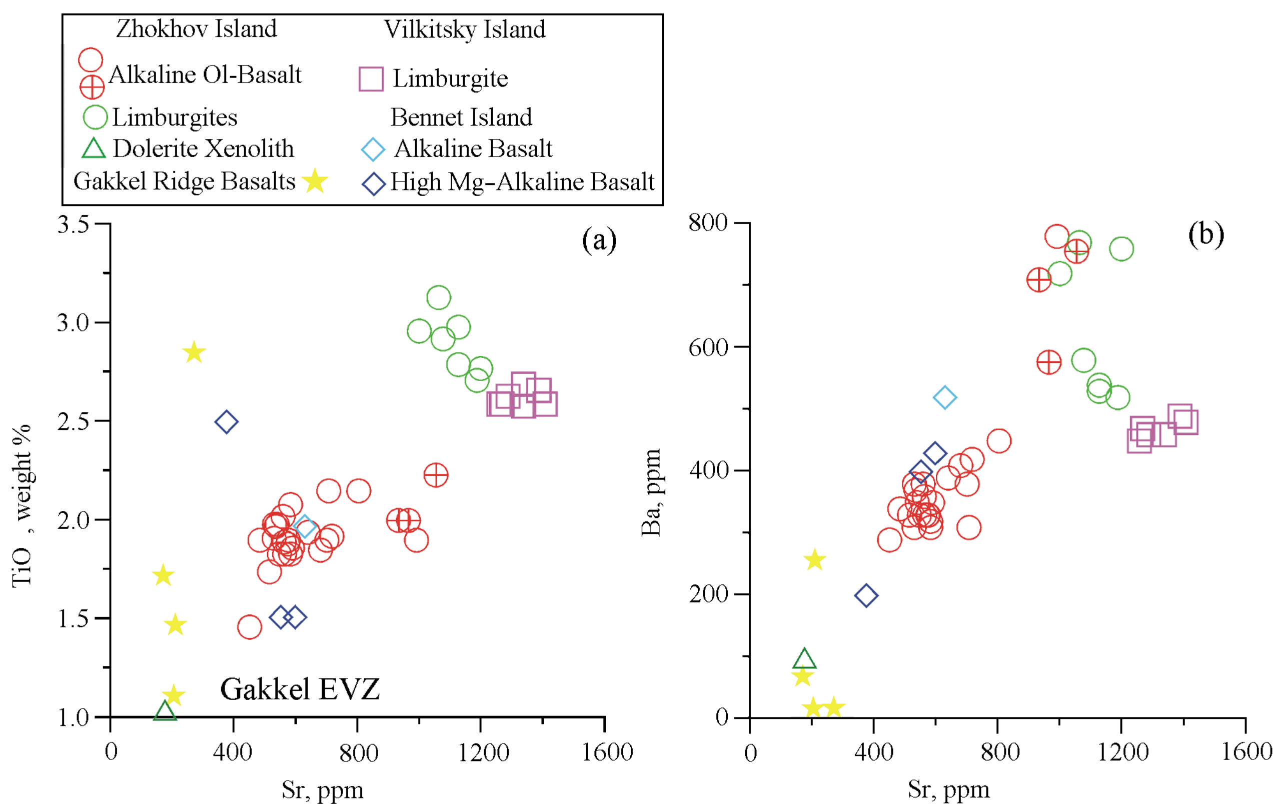

Figure 18. Variations in (a) the Sr vs. TiO_2 and (b) Sr vs. Ba contents in volcanic rocks from the De Long Islands and basalts from the Gakkel Ridge axial zone (after [*Michael et al.*, 2003]). See Figures 3 and 14 for symbol explanations.

Table 3. Trace element contents in rocks from magmatic cpmplexes of De Long Islands

Samples	Locality	Rock Descripition	Cr, ppm	V, ppm	Co, ppm	Ni, ppm	Cu, ppm	Zn, ppm	Rb, ppm	Sr, ppm	Zr, ppm	Y, ppm	Ba, ppm
5-83	Bennet Is.	Alkaline Basalt	88	270	28	31	n.d.	n.d.	18	370	155	28	520
BF-833	Bennet Is.	Mg-Alkaline Basalt	290	155	47	235	n.d.	n.d.	14	340	160	22	200
BF-834	Bennet Is.	Mg-Alkaline Basalt	410	125	52	220	n.d.	n.d.	18	480	420	46	400
BF-835	Bennet Is.	Mg-Alkaline Basalt	5	11	16	5	n.d.	n.d.	20	570	390	45	430
DL-1	Zhokhov Is.	Ol-basalts	n.d.	219	69	210	40	59	13	534	87	n.d.	380
DL-2	Zhokhov Is.	Ol-basalts	n.d.	221	72	223	70	72	13	543	89	n.d.	350
DL-3	Zhokhov Is.	Ol-basalts	n.d.	225	66	198	70	65	13	539	87	n.d.	370
DL-4	Zhokhov Is.	Ol-basalts	n.d.	214	82	243	30	79	17	487	88	n.d.	340
DL-5	Zhokhov Is.	Ol-basalts	n.d.	208	84	623	20	85	21	994	139	n.d.	780
DL-6	Zhokhov Is.	Ol-basalts	n.d.	201	76	356	40	75	13	592	89	n.d.	350
DL-9	Zhokhov Is.	Ol-basalts	n.d.	205	57	151		74	18	586	95	n.d.	320
DL-10	Zhokhov Is.	Ol-basalts	n.d.	211	90	391		81	13	550	89	n.d.	330
DL-11	Zhokhov Is.	Ol-basalts	n.d.	206	107	550	30	73	13	518	83	n.d.	330
DL-12	Zhokhov Is.	Ol-basalts	n.d.	199	80	379	60	70	12	567	86	n.d.	330
DL-16	Zhokhov Is.	Ol-basalts	n.d.	197	69	286	50	78	15	577	88	n.d.	330
DL-17	Zhokhov Is.	Ol-basalts	n.d.	213	87	297	70	81	14	566	90	n.d.	360
DL-18	Zhokhov Is.	Ol-basalts	n.d.	207	78	320	80	75	13	643	101	n.d.	390
DL-19	Zhokhov Is.	Ol-basalts	n.d.	215	59	152		78	14	586	94	n.d.	310
Dl-20a	Zhokhov Is.	Ol-basalts	n.d.	n.d.	n.d.	n.d.	n.d.	n.d.	n.d.	n.d.	n.d.	n.d.	n.d.
DL-21	Zhokhov Is.	Ol-basalts	n.d.	210	64	176	n.d.	77	16	579	95	n.d.	330
DL-22	Zhokhov Is.	Ol-basalts	n.d.	215	58	127	30	81	18	533	95	n.d.	310
DL-23	Zhokhov Is.	Ol-basalts	n.d.	206	82	579	70	74	19	704	116	n.d.	380
DL-24	Zhokhov Is.	Ol-basalts	n.d.	202	79	598	70	69	17	683	111	n.d.	410
DL-25	Zhokhov Is.	Ol-basalts	n.d.	208	82	574	n.d.	70	16	720	115	n.d.	420
DL-26	Zhokhov Is.	Ol-basalts	n.d.	235	63	277	10	91	17	807	124	n.d.	450
DL-27	Zhokhov Is.	Ol-basalts	n.d.	230	69	206	40	64	15	562	93	n.d.	380
DL-28	Zhokhov Is.	Ol-basalts	n.d.	185	129	805	70	90	16	454	79	n.d.	290
DL-36	Zhokhov Is.	Ol-basalts	n.d.	130	40	180	80	100	20	710	160	n.d.	310
DL-13	Zhokhov Is.	Limburgite	n.d.	275	50	170	40	63	15	1066	147	n.d.	770
DL-14	Zhokhov Is.	Limburgite	n.d.	278	58	271	n.d.	69	16	1003	143	n.d.	720
DL-15	Zhokhov Is.	Limburgite	n.d.	264	64	318	n.d.	80	17	1202	150	n.d.	760
DL-32a	Zhokhov Is.	Limburgite	n.d.	160	50	270	n.d.	100	20	1130	180	n.d.	540
DL-33	Zhokhov Is.	Limburgite	n.d.	150	50	280	n.d.	100	20	1130	180	n.d.	530
DL-34	Zhokhov Is.	Limburgite	n.d.	140	50	340	20	100	20	1190	180	n.d.	520
DL-35	Zhokhov Is.	Limburgite	n.d.	130	50	260	10	100	20	1080	190	n.d.	580
DLk-7	Zhokhov Is.	Dolerite	n.d.	211	99	427	120	38	10	180	46	n.d.	100
DLK-1	Zhokhov Is.	Sp-Lherzolite	n.d.	n.d.	n.d.	n.d.	n.d.	n.d.	n.d.	n.d.	n.d.	n.d.	
DLK-2	Zhokhov Is.	Sp-Lherzolite	n.d.	80	80	1950	110	90	30	30	110	n.d.	130
DLK-4	Zhokhov Is.	Sp-Lherzolite	n.d.	80	90	2120	10	90	30	10	100	n.d.	120
DLK-5	Zhokhov Is.	Sp-Lherzolite	n.d.	n.d.	n.d.	n.d.	n.d.	n.d.	n.d.	n.d.	n.d.	n.d.	n.d.

Table 3. Continued

Samples	Locality	Rock Descripition	Cr, ppm	V, ppm	Co, ppm	Ni, ppm	Cu, ppm	Zn, ppm	Rb, ppm	Sr, ppm	Zr, ppm	Y, ppm	Ba, ppm
DLK-3	Zhokhov Is.	Sp-Lherzolite	n.d.	n.d.	n.d.	n.d.	n.d.	n.d.	n.d.	n.d.	n.d.	n.d.	n.d.
DL-38	Vilkitski Is.	Limburgite	n.d.	150	50	160	30	100	10	1340	200	n.d.	460
DL-39	Vilkitski Is.	Limburgite	n.d.	140	50	140	n.d.	100	10	1340	190	n.d.	460
DL-40	Vilkitski Is.	Limburgite	n.d.	150	50	170	10	100	10	1290	200	n.d.	460
DL-41	Vilkitski Is.	n Limburgite	n.d.	140	50	170	10	100	10	1260	200	n.d.	450
DL-42	Vilkitski Is.	Limburgite	n.d.	150	50	170	n.d.	100	10	1410	200	n.d.	480
DL-43	Vilkitski Is.	Limburgite	n.d.	140	50	160	10	100	10	1270	200	n.d.	470
DL-45	Vilkitski Is.	Limburgite	n.d.	150	50	140	50	100	10	1390	200	n.d.	490

Note: n.d. – not determined.

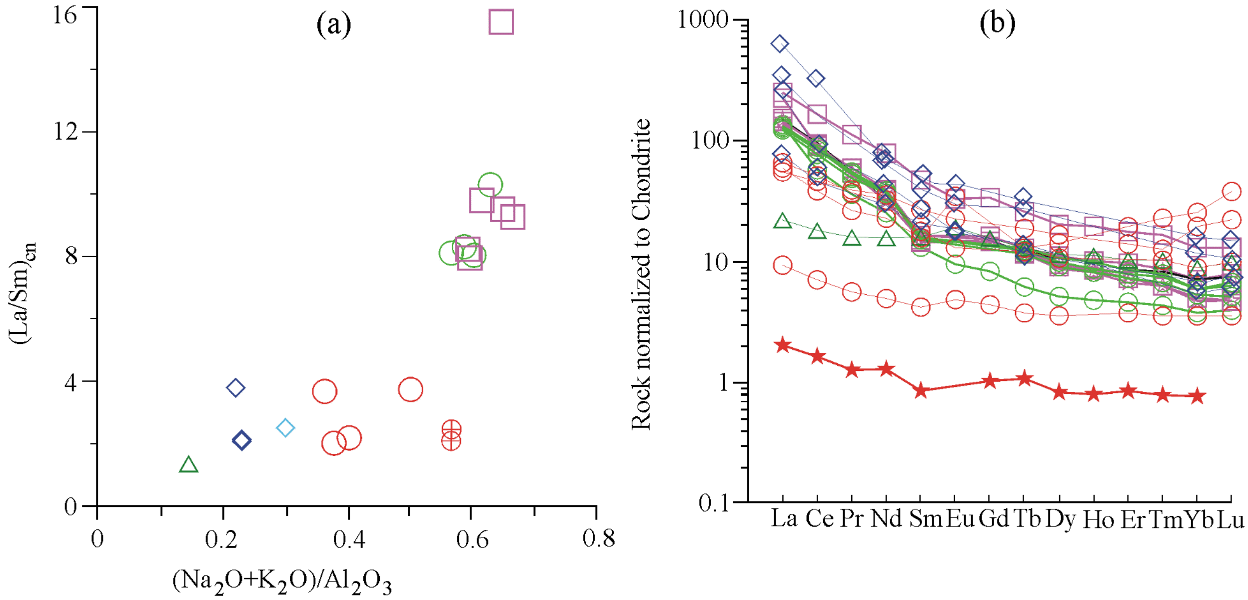

Figure 19. Variations in (a) the degree of enrichment $(La/Sm)_{cn}$ vs. the $(Na_2O + K_2O)/Al_2O_3$ ratio of volcanic rocks from the De Long Islands and (b) their chondrite-normalized [*Sun and McDonough,* 1989] REE patterns. See Figures 3 and 14 for symbol explanations.

in LREE notably more significantly ($(La/Sm)_{cn}$ = 8.0–15.6) than the accompanying alkaline olivine basalts ($(La/Sm)_{cn}$ = 2.0–3.8). Figure 19a also demonstrates that both the alkaline and the magnesian alkaline olivine basalts from Bennett Island have $(La/Sm)_{cn}$ ratios equal to those of the alkaline basalts from Zhokhov Island (2.5–3.8). The dolerite from the xenolith suite of Zhokhov Island exhibits the lowest $(La/Sm)_{cn}$ ratio equal to 1.4. Thus, it follows that all petrographic types of the rocks are characterized by a clearly pronounced enriched character of REE distribution (Table 4, Figures 19a, 19b). The alkaline olivine basalts of Zhokhov and Bennett islands display a general increase in the REE contents with an increase in the degree of fractionation. The flattest (although with a discernible tendency toward enrichment) REE pattern in Figure 19b is that of sample of the dolerite xenolith. As follows from Figure 19b, LREE enrichment is also characteristic of the spinel lherzolites of mantle xenoliths.

It can be concluded that the geochemical features of volcanic rocks from Bennett, Zhokhov, and Vil'kitskii islands make them similar to volcanics in within-plate magmatic provinces, including the basalts of oceanic islands (OIB) and continental rifts. It is pertinent to emphasize that within-plate volcanic products in the central part of the De Long Islands also show geochemical similarities with the young alkaline basalts of volcanic centers in the continental fringing of the Laptev Sea shelf southeast of the sea: Balagan-Tas Volcano in the Chersky Range, Moma Rift, and the Quaternary (?) dike complex at the Viliga River in the Sea of Okhotsk area, which contain spinel lherzolite xenoliths [*Grachev,* 1999]. The data presented in Figures 12–19 do not rule out the possibility that the alkaline basalts of Bennett Island were produced by a parental melt whose composition was similar to that of the parental melt of the olivine alkaline basalts in Zhokhov Island. The dolerite of the crustal xenolith form Zhokhov Island has many compositional parameters (the Sr and K_2O concentrations and the $(La/Sm)_{cn}$ ratio] close to the analogous values for enriched MORB basaltoids, although the former rock is poorer in TiO_2 and Na_2O. Earlier, analysis of the distribution of major and incompatible elements in basalts from Bennett Island led to the conclusion that these rocks could be close to continental flood basalts or rift-related alkaline basalts in continental margins, and the magnesian alkaline basalts are close to the rocks of mildly alkaline series in continental rifts or OIB [*Fedorov et al.,* 2002].

The geochemistry of spinel lherzolites from the De Long Islands make these rocks similar to peridotites, i.e., the material of the primitive (undepleted) mantle. This follows from the MgO/SiO_2 and Al_2O_3/SiO_2 ratios of these rocks: 1.19–1.25 and 0.07–0.08, respectively. Spinel lherzolites similar to those found on Zhokhov and Vil'kitskii islands are the most ubiquitous rocks of mantle xenoliths in areas of within-plate magmatism in both continents and oceanic islands, such as Victoria in Australia and Hawaii [*Frey and Green,* 1974; *Irving,* 1980; *Jackson and Wright,* 1970].

Isotopic Geochemistry of the Magmatic Complexes in Bennett, Zhokhov, and Vil'kitskii Islands

The K–Ar ages of the olivine alkaline basalts, limburgites, and dolerite xenolith from Zhokhov and Vil'kitskii islands were published in [*Bogdanovskii et al.,* 1992] and are presented in Table 5. Judging from available data, limburgite volcanism on Vil'kitskii Island (0.89–0.4 Ma) can be corre-

Table 4. REE contents in igneous rocks from De Long Islands

Samples	Locality	Rock Descripition	La	Ce	Pr	Nd	Sm	Eu	Gd	Tb	Dy	Ho	Er	Tm	Yb	Lu	$(La/Sm)_{cn}$
5-83	Bennet Is.	Alkaline Basalt	33	75	n.d.	38	8.4	2.6	n.d.	1.4	n.d.	n.d.	n.d.	n.d.	2.9	0.42	2.54
BF-833	Bennet Is.	Alkaline Basalt	17	36	n.d.	21	5.2	1.7	n.d.	0.74	n.d.	n.d.	n.d.	n.d.	2	0.31	2.11
BF-834	Bennet Is.	Alkaline Basalt	32	52	n.d.	26	5.4	1.7	n.d.	0.97	n.d.	n.d.	n.d.	n.d.	1.5	0.22	3.83
BF-835	Bennet Is.	Alkaline Basalt	37	77	n.d.	43	11	3.7	n.d.	2	n.d.	n.d.	n.d.	n.d.	4.4	0.6	2.17
DL-3	Zhokhov Is.	Ol-basalts	2.2	4.3	0.53	2.3	0.64	0.28	0.9	0.14	0.9	0.06	0.62	0.09	0.6	0.09	2.22
DL-5	Zhokhov Is.	Ol-basalts	14	23.4	2.5	10.6	2.4	2	2.4	0.48	3.6	1	3.2	0.58	4.3	0.96	3.77
DL-19	Zhokhov Is.	Ol-basalts	13	28	3.7	16.5	4.1	1.3	4.8	0.7	4.2	0.84	2.3	0.32	3.3	0.56	2.05
DL-22	Zhokhov Is.	Ol-basalts	15.5	31.2	3.5	15	2.7	0.75	3	0.45	2.7	0.6	1.7	0.26	1.5	0.25	3.71
DL-32a	Zhokhov Is.	Limburgite	32	35	3.4	11.8	2	0.55	1.7	0.23	1.3	0.27	0.76	0.11	0.64	0.1	10.33
DL-33	Zhokhov Is.	Limburgite	29	47	4.6	17.1	2.3	2.5	3	0.43	2.3	0.46	1.2	0.17	0.9	0.13	8.14
DL-34	Zhokhov Is.	Limburgite	31	54	5.2	17.8	2.4	3.8	3.5	0.48	2.7	0.56	1.4	0.2	1	0.17	8.34
DL-35	Zhokhov Is.	Limburgite	30	51	5	17	2.4	2.2	3	0.46	2.5	0.49	1.3	0.19	1	0.16	8.07
DLk-7	Zhokhov Is.	Dolerite xenolith	5.2	11	1.5	7.3	2.42	1.11	3.2	0.48	2.9	0.63	1.7	0.26	1.5	0.25	1.39
DLK-1	Zhokhov Is.	Sp-Lherzolite	0.48	1	0.12	0.6	0.13	0.13	0.21	0.04	0.21	0.05	0.14	0.02	0.13	0.12	2.38
DL-38	Vilkitski Is.	Limburgite	7.3	11	1.2	4.1	0.59	2.5	0.9	0.17	1.4	0.43	1.7	0.37	3.1	0.77	7.99
DL-39	Vilkitski Is.	Limburgite	36	55	5.6	18.3	2.5	3.2	3.3	0.48	2.8	0.57	1.6	0.22	1.2	0.2	9.3
DL-40	Vilkitski Is.	Limburgite	32	52	4.9	17.7	2.5	2.9	3.1	0.43	2.2	0.46	1.1	0.16	0.8	0.12	8.26
DL-41	Vilkitski Is.	Limburgite	53	55	5.1	17.7	2.2	3.3	3	0.43	2.3	0.48	1.2	0.16	0.85	0.12	15.55
DL-42	Vilkitski Is.	Limburgite	35	58	5.2	14.8	2.3	3.3	3	0.45	2.7	0.56	1.4	0.21	1.2	0.19	9.82
DL-43	Vilkitski Is.	Limburgite	34	57	5.1	14.7	2.3	3.3	3	0.44	2.4	0.5	1.3	0.19	1	0.16	9.54
DL-49	Vilkitski Is.	Limburgite	59	101	10.6	36.6	7.2	1.9	6.9	0.96	5.1	1.1	2.9	0.42	2.2	0.33	5.29

Note: n.d. – not determined; normalization by [*Sun and McDonough,* 1989]; concentrations are given in ppm.

Table 5. Results of K-Ar dating

Samples	Locality	Rock Descripition	$^{36}Ar/^{40}Ar$ measured	^{40}Ar atm.,%	K_2O, wt. %	T, m.y.
5-83	Bennet Is.	Alkaline Basalt				106
BF-833	Bennet Is.	Mg-Alkaline Basalt				109
BF-834	Bennet Is.	Mg-Alkaline Basalt				110
BF-835	Bennet Is.	Mg-Alkaline Basalt				124
DL-1	Zhokhov Is.	Ol-basalts	0.00301	89	1.56	1.7
DL-2	Zhokhov Is.	Ol-basalts	0.00278	82.8	1.62	1.87
DL-3	Zhokhov Is.	Ol-basalts	0.002	59	1.59	1.57
DL-9	Zhokhov Is.	Ol-basalts	0.00236	69.7	1.18	1.6
DL-18	Zhokhov Is.	Ol-basalts	0.00249	73.5	1.3	5.62
DL-19	Zhokhov Is.	Ol-basalts	0.00277	81.8	1.24	2.33
Dl-20a	Zhokhov Is.	Ol-basalts	0.0025	73.9	1.54	2.96
Dl-20b	Zhokhov Is.	Ol-basalts	0.00189	55.9	1.54	3.3
DL-21	Zhokhov Is.	Ol-basalts	0.00292	86.3	1.34	0.53
DL-22a	Zhokhov Is.	Ol-basalts	0.00251	74.1	1.2	1.83
DL-22b	Zhokhov Is.	Ol-basalts	0.00245	72.4	1.2	1.68
DL-26a	Zhokhov Is.	Ol-basalts	0.00322	95.2	1.52	5.1
DL-26b	Zhokhov Is.	Ol-basalts	0.00318	94.1	1.52	6.1
DL-15	Zhokhov Is.	Limburgite	0.00295	87.2	2.06	3.22
DL-32a	Zhokhov Is.	Limburgite	0.00224	66.2	2.68	3.27
DL-32b	Zhokhov Is.	Limburgite	0.00204	60.3	2.68	4.21
DL-33	Zhokhov Is.	Limburgite	0.00268	79.3	2.38	3.68
DL34a	Zhokhov Is.	Limburgite	0.00298	88.1	2.28	1.9
DL34b	Zhokhov Is.	Limburgite	0.00303	89.5	2.28	1.88
DLk-7 light fr.	Zhokhov Is.	Dolerite	0.000582	17.3	0.56	152.3
DLk-7 heavy fr.	Zhokhov Is.	Dolerite	0.000835	24.6	0.21	99.5
DL-38	Vilkitski Is.	Limburgite	0.00319	94.2	2.24	0.4
DL-39	Vilkitski Is.	Limburgite	0.00327	96.7	2.34	0.4
DL-42a	Vilkitski Is.	Limburgite	0.00322	95.1	2.39	0.87
DL-42b	Vilkitski Is.	Limburgite	0.00298	88.1	2.39	0.89

Note: Results for basalts from Bennet Island given as in [*Fedorov et al.,* 2002].

lated with the late evolutionary stages of the olivine alkaline basalt association on Zhokhov Island (6.1–0.4 Ma) but was significantly briefer. The K–Ar ages of the rocks composing the volcanic complex of the Bennett Island were reported in [*Fedorov et al.,* 2002] and are 106 Ma for the alkaline basalts composing stratified lava sheets and 109–124 Ma for the magnesian alkaline basalts of the lava flows and cones.

The leucocratic and melanocratic fractions of dolerite from the crustal xenolith suite were dated by the K–Ar method at 152±5 and 100±3 Ma, respectively [*Bogdanovskii et al.,* 1992]. Considering that the sample shows traces of secondary alterations and that plagioclase (which is abundant in the leucocratic fraction) is prone to entrap excess radiogenic Ar (whose content is higher in the leucocratic fraction), preference should be given to the younger age value, which was obtained for melanocratic minerals. It is, however, impossible to unambiguously correlate this value with any geologic event without employing additional information. Provisionally we assumed that the age of this dolerite is 100±3 Ma, but it cannot be ruled out that part of the radiogenic Ar was lost during reheating, so that the actual age of the rock should be much older.

There are, thus, good reasons to believe that volcanic activity at the De Long Islands was prone to become systematically younger from the offshore margin of the Laptev Sea shelf (Bennett Island—Early–Late Cretaceous boundary) toward its inner parts (Zhokhov Island) and farther southeastward (Vil'kitskii Island—Quaternary, Pleistocene). Proceeding from the assumption that the dolerite xenolith has isotopic and geochemical characteristics classifying it as a fragment of the crustal material of the Laptev Sea shelf, it should be assumed that this material has an early Cretaceous age.

The sample selected for the isotopic study of the mantle xenoliths was the least altered and the most coarse-grained rock (sample DLK-1), which consisted of olivine (65%), orthopyroxene (20%), clinopyroxene (12%), and spinel (3%). The temperature of characteristic mineral equilibria in this rock was evaluated by geothermometers at 1211°C, which corresponded to the highest value among all of the xenoliths. This led us to suggest that the material of the xenolith was not significantly affected by postcrystallization processes. The Nd isotopic composition and the $^{147}Sm/^{144}Nd$ ratios were determined in the whole rock of sample DLK-1, its rock-forming Ol, Cpx, and Opx, and in HCl leachate and residue after leaching (Table 6). These

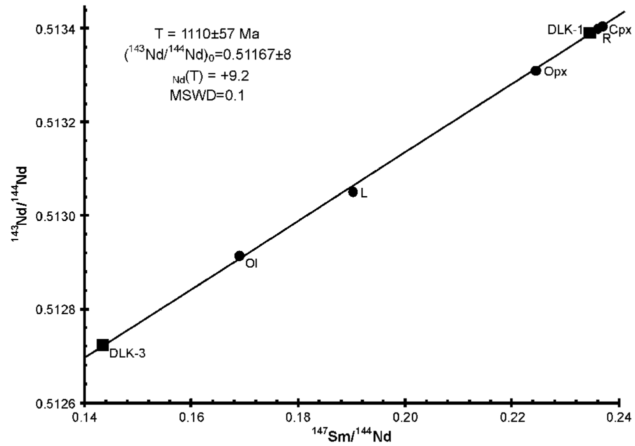

Figure 20. Sm–Nd isochron diagram for spinel lherzolite (sample DLK-1). The diagram demonstrates the results obtained on a whole-rock sample, monomineralic fractions, HCl leachate (L), residue after leaching (R), and a composite sample of a number of small spinel lherzolite xenoliths separated from a single rock block (sample DLK-3). Although the point corresponding to the latter sample was not used in calculating the parameters of the isochron, this point also plots (within the analytical error) on the isochron, a fact pointing to the equality of the initial Nd isotopic ratios in all samples.

data defined an isochron, whose slope corresponded to an age of 1110±57 Ma at an initial Nd isotopic ratio of 0.51167±8, MSWD = 0.1 (Figure 20). Note that the same mineral isochron passes through the point corresponding to averaged sample DLK-3 (a composite sample of a number of small spinel lherzolite xenoliths obtained from a single rock fragment). Compared with sample DLK-1, this sample is notably higher in Sm and Nd at a much lower Sm/Nd ratio. Obviously, these geochemical differences in the ancient mantle material were caused by its local heterogeneity. It should be emphasized that this compositional heterogeneity (at 1.11 Ga) was not originally coupled with any isotopic heterogeneity but eventually resulted in remarkable differences (for example, in the Nd isotopic compositions) between samples DLK-1 and DLK-3 (compare Figures 20 and 21). The possible geochemical consequences of this isotopic heterogeneity are discussed below.

The isotopic characteristics of spinel lherzolites from the De Long Islands and their host within-plate volcanic rocks allowed us to conclude that the young (6.1–0.4 Ma) volcanic rocks of this sector of the Arctic basin carry xenoliths of ancient (1.11 Ga) mantle material. Available data provide grounds to believe that mantle xenoliths from Zhokhov and Vil'kitskii islands are fragments of mantle rocks whose Nd and Sr isotopic composition corresponded to the depleted mantle. This material was not involved in the melting processes over at least the past 1.11 Ga.

The close spatial association of alkaline basalts and limburgites in the central part of the De Long Islands (on Zhokhov Island) suggests their genetic similarity and a common magmatic history. Data on the Sr and Nd isotopic composition of the volcanic rocks (Table 6) make it possible to reconstruct more confidently both the nature of the mantle sources of magmatism that gave rise to these rocks and the evolution of the parental melts. These rocks contain less radiogenic Nd and more radiogenic Sr than in the source of MORB, with the most radiogenic Sr detected in the dolerite of the crustal xenolith from Zhokhov Island.

The data presented above indicate that the alkaline basalts and limburgites of Bennett, Zhokhov, and Vil'kitskii islands have similar Sr and Nd isotopic composition and, thus, can be regarded as the derivatives of a single magmatic melt, which was derived by the melting of a mantle source (or sources) having similar Sr and Nd isotopic signatures, with the $^{87}Sr/^{86}Sr$ ratio varying within 0.0006 and ε_{Nd} within two units. However, when the Sr isotopic compositions of these rocks are examined more closely, they show small but systematic differences. These differences can be accounted for by (1) the insignificant isotopic heterogeneity of the source, (2) the contamination of the melt with the material of the oceanic crust, or (3) the interaction of the magmatic source with seawater. Below these three possibilities will be considered in the reverse order.

All of the rocks used in our research were very fresh, without any mineralogical or geochemical traces of interaction with seawater. An independent argument for the absence of this interaction is furnished by the identity of the Nd and Sr isotopic composition of the acid leachates and residues after the preliminary leaching of the samples.

The alkaline olivine basalts contain systematically slightly higher concentrations of radiogenic Sr than those in the limburgites (Figure 22a), a fact that can, in principle, be regarded as an indication of the contamination of the parental melts. Obviously, this contaminant could be the rocks that occur as crustal xenoliths in dolerites and the carbonatized volcanic rocks found on Zhokhov Island. These rocks could

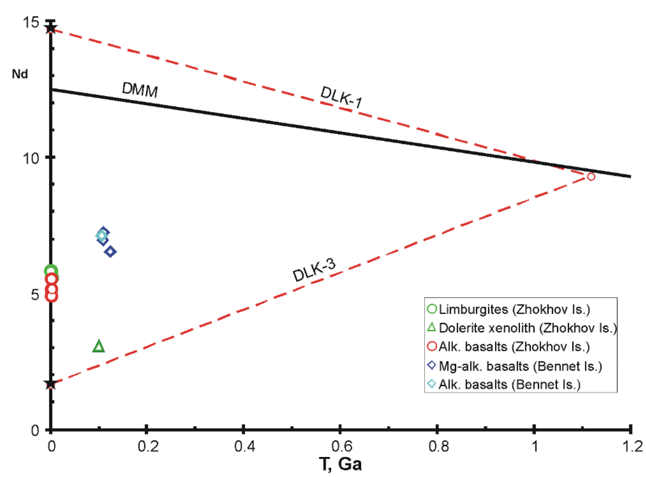

Figure 21. Evolution of the Nd isotopic composition in the spinel lherzolite mantle xenoliths DLK-1 and DLK-3 and in the crustal xenolith DLK-7 in comparison with data on the alkaline basalts and limburgites. The solid line corresponds to the hypothetical DMM mantle source [*Zindler and Hart,* 1986].

Table 6. Rb-Sr and Sm-Nd isotopic data of igneous rocks from De Long Islands

Sample	Location	Desc.	Rb, ppm	Sr, ppm	$^{87}Sr/^{86}Sr$	Sm, ppm	Nd, ppm	$^{147}Sm/^{144}Nd$	$^{143}Nd/^{144}Nd$	$\varepsilon_{Nd}(0)$	$\varepsilon_{Nd}(T)$
DLK-3	Zhokhov Is.	Sp-Lherzolite			0.70394	0.657	2.776	0.1433	0.512723	1.7	9.32
DLK-1	Zhokhov Is.	Sp-Lherzolite				0.1455	0.375	0.2345	0.513392	14.7	9.33
DLK-1 L	Zhokhov Is.	HCl-leaching				0.0057	0.0182	0.1902	0.513052	8.1	9.03
DLK-1 R	Zhokhov Is.	Restite				0.240	0.616	0.2360	0.513400	14.9	9.27
DLK-1 Cpx	Zhokhov Is.	Cpx				1.126	2.877	0.2369	0.513405	15.0	9.24
DLK-1 Opx	Zhokhov Is.	Opx				0.016	0.0432	0.2244	0.513311	13.1	9.19
DLK-1 Ol	Zhokhov Is.	Ol				0.0036	0.0129	0.1690	0.512915	5.4	9.40
Dl-39	Zhokhov Is.	Limburgite	10*	1340*	0.70303		53.9	0.083*	0.512936	5.8	5.83
DL-15	Zhokhov Is.	Limburgite	17*	1202*	0.70311		46.6	0.10*	0.512922	5.5	5.59
DL-5	Zhokhov Is.	Ol basalt	21*	994*	0.70360		38.3	0.137*	0.512920	5.5	5.52
DL-22	Zhokhov Is.	Ol basalt	18*	533*	0.70362		16.6	0.109*	0.512889	4.9	4.92
DL-19	Zhokhov Is.	Ol basalt	14*	586*	0.70336		18	0.150*	0.512902	5.2	5.17
DLK-7	Zhokhov Is.	Xenolith Dolerite	10*	180*	0.70562		9.8	0.200*	0.512797	3.1	3.06
5-83	Bennet Is.	Alkaline Basalt	18*	632.8	0.70351	8.03	35.51	0.1367	0.512961	6.3	7.11
BF-833	Bennet Is.	Mg-Alkaline Basalt	14*	379.1	0.70377	3.9	16.01	0.1471	0.512959	6.3	6.95
BF-834	Bennet Is.	Mg-Alkaline Basalt	18*	554.9	0.70375	5.8	27.46	0.1277	0.512960	6.3	7.25
BF-835	Bennet Is.	Mg-Alkaline Basalt	20*	601.2	0.70346	14.8	64.68	0.1387	0.512926	5.6	6.54

Note: * – concentrations by data of NAA, others – isotopic dilution.

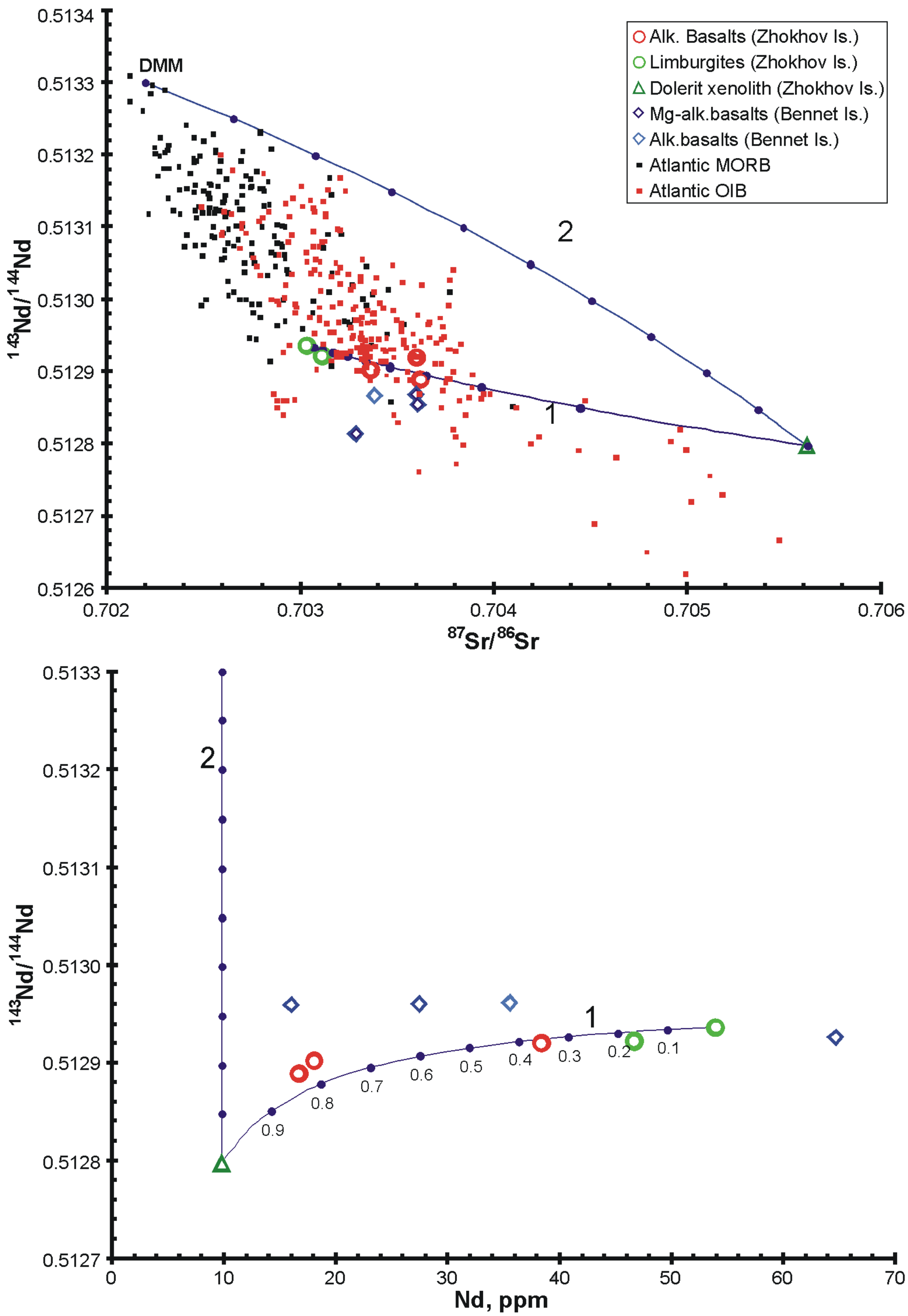

Figure 22. Illustration for the model of melt contamination with oceanic crustal material. The contaminant in both plots is the dolerite xenoliths (sample DLK-7) material. The original melt compositions correspond to limburgite DL-39 for line 1 and has Nd and Sr isotopic characteristics analogous to those of the hypothetical DMM source with contents of [Sr] = 130 ppm and [Nd] = 10 ppm. Ticks on mixing lines are spaced 10% increment in the contaminant amount.

be fragments of the ancient (Mesozoic ?) crustal material of the Laptev Sea shelf that was altered during interaction with seawater. Figure 22 demonstrates the results obtained by simulating the mixing process with the aim of evaluating the degree of contamination. The solid line demonstrates the model of mixing for a melt corresponding in composition to limburgite DL-39 and the material of the dolerite xenolith. As can be see from the plots in Figures 22a and 22b, all data points of alkaline basalts are quite well fitted by the model. However, the content of the contaminating oceanic crustal material should amount to 60% (relative to the original amount of the melt) in Figure 22a and comes as high as 80% in Figure 22b. Thus, both values seem to be unrealistic overestimates. They were caused by the fact that the Sr and Nd concentrations in xenolith DLK-7 are five- to seven-fold lower than in limburgite DL-39. For the contamination model to be plausible, the contaminant should contain manyfold higher Nd and Sr concentrations than those in xenolith DLK-7.

As is seen in Figure 22a, the Sr and Nd isotopic ratios in the limburgites and alkaline olivine basalts are close to those in the enriched (plume-related) sources of MORB or OIB. The genesis of these enriched (with respect to the DMM source) rocks was a matter of heated discussions over the past decades and is believed to be somehow related to the recycling of the crustal material: via either the direct recycling of the isotopically anomalous material or the recycling of chemically enriched material that eventually gives rise to isotopic anomalies in the mantle. A comprehensive review on this problem was published in [*Hofmann,* 2003].

Figure 22a demonstrates mixing lines for a MORB melt from the hypothetical DMM source [*Zindler and Hart,* 1986] and a potentially possible crustal contaminant (represented by sample DLK-7). The Nd and Sr isotopic ratios in the limburgites and alkaline olivine basalts are in apparent conflict with the hypothesis of mixing of melts from the DMM source and oceanic crustal material.

The genesis of the isotopic ratios observed in the limburgites and alkaline basalts of the De Long Islands can be understood from Figure 21. The present variations in the Nd isotopic ratios in spinel lherzolite nodules are quite broad: from +1.7 to +14.7 $\varepsilon_{\mathrm{Nd}}$ units. This isotopic heterogeneity was caused by the *in-situ* enrichment of ^{143}Nd in originally (at 1.11 Ga) isotopically homogeneous material as a natural consequence of the chemical heterogeneity of this material, including an uneven distribution of the Sm/Nd ratio. If the source of the melts that produced the De Long volcanics was characterized by a chemical heterogeneity similar to that in xenoliths of the analyzed samples (DLK-1 and DLK-3), then the occurrence of local domains enriched in lithophile elements, including LREE, for a long time (during which the Sm/Nd ratio decreased) should have inevitably brought about the development of isotopically enriched characteristics of these rocks. The melting of these isotopically and chemically anomalous zones could have simultaneously produce chemically enriched melts with lower Nd isotopic ratios.

In a Sm/Nd vs. ^{143}Nd/^{144}Nd diagram, all of the rocks from the De Long Islands plot within the field of basalts belonging to the plume association of the Mid-Atlantic Ridge (Figure 23), which have the lowest Sm/Nd ratios. Along with the geochemical data presented above, this led us to think that the volcanic complexes were produced by plume-related magmatism. Figure 23 also demonstrates that the limburgites are enriched in LREE (have lower Sm/Nd ratios) more strongly than the alkaline olivine basalts.

Conclusion

Analyzing the spatial distribution of the geochemical types of volcanic complexes of different ages within the sector of the Arctic basin discussed in this paper enabled us to reproduce the geochemical nature of the upper mantle beneath the central part of the Laptev Sea continental shelf and the nature of the deep-seated mantle sources that produced the within-plate magmatic melt over the past 120 m.y.

Isotopic data testify that the spinel lherzolites entrained as xenoliths by magmas in the De Long Islands could not be captured in the mantle sources whose melting gave rise to the Mesozoic and Cenozoic magmatism on Bennett, Zhokhov, and Vil'kitskii islands. Available data indicate that the material represented by these xenoliths was not involved in melting processes over at least the past 1.11 Ga. At 1.11 Ga, the mantle material whose fragments are the spinel lherzolites was compositionally, but not isotopically, heterogeneous. However, this initial compositional heterogeneity triggered the development of isotopic heterogeneity in the same mantle material (see above: samples DLK-1 and DLK-3).

Mantle xenoliths with isotopic characteristics similar to those of the spinel lherzolites from the De Long Islands are known in the eastern and central parts of the Asian continent: these are garnet peridotites in the Mir kimberlite pipe in Yakutia and garnet and spinel peridotites from the Vitim Highlands and Mongolia [*Ionov,* 1988; *Ionov and Jagoutz,* 1988; *Kovalenko et al.,* 1990]. It is possible that the De Long Islands mark the northernmost limit of the Asian mantle anomaly [*Ionov and Jagoutz,* 1988; *Zhuravlev et al.,* 1991], which is located at depth of 45–75 km and has not been involved in melting processes since 1 Ga.

As was demonstrated above, petrological evidence indicates that the weakly depleted mantle source material represented by the spinel lherzolites is localized beneath the central part of the De Long Islands at a depth of approximately 60 km, and, thus, the sources of the parental melts of the alkaline basalts and limburgites should have been situated at even greater depths. A. E. Ringwood believed [*Ringwood,* 1975] that the melts parental for nephelinite (in our case, for the limburgite) series are derived at greater depths than the melts to which alkaline olivine basalts are related. At the same time, the two within-plate magmatic series were, perhaps, generated by the partial melting of a single mantle source, with limburgite–nephelinite and olivine alkaline basaltic melts produced at low and high degrees of melting, respectively. This scenario for the origin of the two major types of magmatic series in the De Long Islands seems to be the most plausible, because the data presented above demonstrate similarities between the isotopic–geochemical charac-

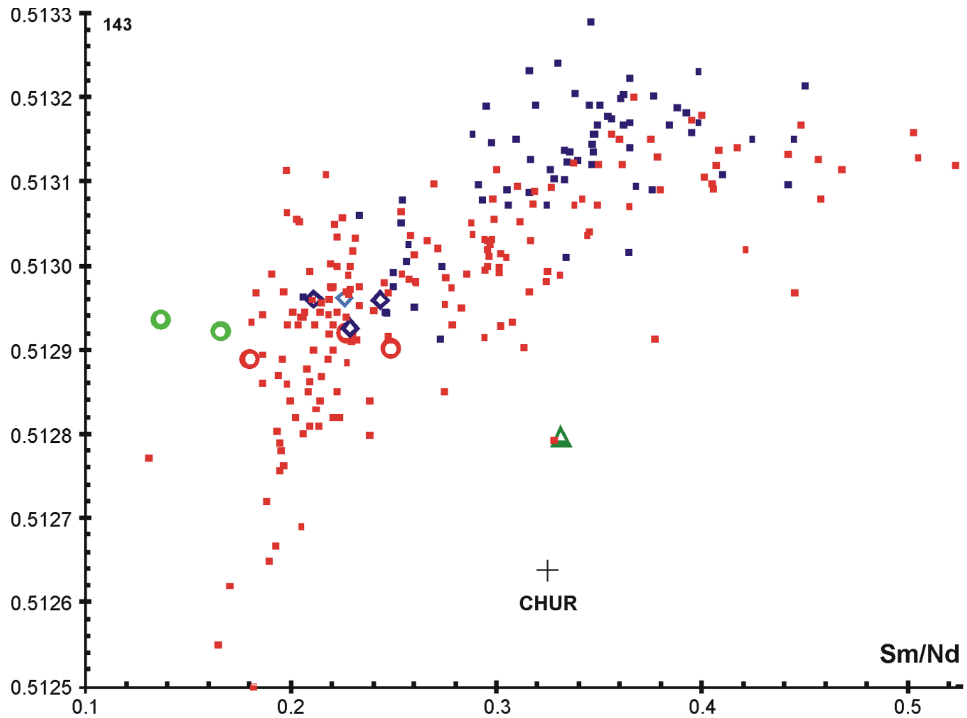

Figure 23. Correlation between the ^{143}Nd/^{144}Nd and Sm/Nd ratios in volcanic rocks from the De Long Islands. Shown for comparison are the compositions of Atlantic MORB and OIB.

teristics of the limburgites and alkaline olivine basalts. The enrichment of the limburgites in incompatible elements (for example, Sr and K) relative to the alkaline olivine basalts could hardly be caused by the fractionation of a common parental melt, because this scenario is at variance with the much more stronger LREE enrichment in the limburgites than in the alkaline olivine basalts (more than fourfold in some samples, see above).

It is quite difficult to interpret the genesis of the dolerite from the crustal xenolith suite on Zhokhov Island because of the ambiguity of the age estimates for this rock. If its age is 100±3 Ma, it is reasonable to assume that the dolerite was produced synchronously with the alkaline basalts of Bennett Island and, thus, composed, together with them, the Mesozoic mafic basement of the Laptev Sea shelf. This interpretation implies that the magmatic evolution of the continental shelf in the Laptev Sea at the Early and Late Cretaceous boundary was participated by at least two geochemically distinct mantle sources, one of which was responsible for the formation of plume-type melts (basalts of Bennett Island), and the other produced the parental melts of enriched MORB (dolerite from the crustal xenolith suite of Zhokhov Island). The geochemical similarities between the dolerite and enriched MORB is confirmed by similarities of some compositional parameters of the dolerite (see Figures 18a 18b) and basalts from the Gakkel Ridge. According to [*Michael et al.,* 2003], the latter rocks are generally enriched more significantly than MORB in incompatible elements.

An alternative interpretation of the origin of the dolerite from xenoliths on Zhokhiv Island is based on the assumption that the radiogenic Ar contained in this rock was partly lost due to reheating, and the actual age of the dolerite is much older than 100 Ma. Then it should be assumed that the dolerite xenolith represents the ancient continental crust of the Laptev Sea shelf. A rough idea about its composition is provided by the Lower Paleozoic rocks of Bennett Island: Cambrian mudstones with trilobites and Ordovician mudstones and sandstones. The association of Paleozoic sedimentary and metasedimentary rocks can also include the quartzites found among xenoliths on Zhokhov Island.

The isotopic data presented above suggest that the alkaline basalts and limburgites of Bennett, Zhokhov, and Vil'kitskii islands could be generated by magmatic melts derived from a common mantle source or isotopically similar mantle sources. Within-plate melts with isotopic–geochemical signatures of the limburgites and alkaline olivine basalts from the De Long Islands could be produced by a mantle source whose chemical heterogeneity was comparable with the heterogeneity of the shallower sitting mantle material represented by spinel lherzolite mantle xenoliths on Zhokov and Vil'kistkii islands. The melting of such a mantle material, which included local zones enriched in lithophile elements, gave rise to chemically enriched melts with lower Nd isotopic ratios.

The results obtained by simulating the mixing process presented above are in conflict with the earlier hypothesis that the melts parental for the alkaline olivine basalts were contaminated with the material of the melanocratic basement of the Laptev Sea shelf [*Bogdanovskii et al.,* 1992].

It is, thus, reasonable to believe that the magmatic system in which the within-plate volcanic associations of Bennett, Zhokhov, and Vil'kitskii islands were formed evolved without any notable chemical interaction with older crustal material.

As follows form the same model simulations, the Nd and Sr isotopic ratios observed in the limburgites and alkaline olivine basalts rule out the possibility that their parental melts mixed with the material of the DMM source. This conclusion implies that Mesozoic–Cenozoic magmatism at the De Long Islands was controlled exclusively by the melting of deep-seated enriched mantle sources, without involvement of shallower sources that produced N-MORB.

Judging from the isotopic–geochemical characteristics of volcanic rocks of the De Long Islands, these rocks are compositionally close to the most strongly enriched basaltoids in anomalous (plume) MAR segments or in oceanic islands (OIB). Hence, the alkaline basalts and limburgites of Bennett, Zhokhov, and Vil'kitskii islands can be classed with the products of plume magmatism. It is worth noting that the degree of enrichment of these rocks systematically increases from the alkaline basalts of Bennett Island to the alkaline olivine basalts and limburgites of Zhokhov Island and further to the limburgites of Vil'kitskii Island. This fact suggests that magmatism in the central part of the De Long Islands was contributed more significantly by the enriched mantle component as compare with North-West periphery of archipelago.

Taking into account all considerations presented above, the following scenario can be proposed for the evolution of magmatism and its compositional characteristics in this segment of the East Arctic basin (Figure 24).

1. The Mesozoic mafic basement of the Laptev Sea shelf was produced at the boundary between the Early and Late Cretaceous. The origin of the magmatic complex during this stage of the geological history of the Laptev Sea shelf was participated by at least two geochemically distinct mantle sources. One of them gave rise to plume-type melts (the basalts of Bennett Island, which are the oldest magmatic rocks in this area), and the other was responsible for the origin of melts parental for the enriched MORB (dolerite from the crustal xenolith suite of Zhokhov Island). In the alternative variants, the dolerites should be ascribed to the material of the ancient continental crust of the Laptev Sea shelf, with this crustal material also including the Early Paleozoic sedimentary rocks of Bennett Island and quartzites of the crustal xenolith suite of Zhokhov Island.

2. After a fairly long (approximately 100 m.y.) interlude in the magmatic activity, the late stage magmatic of magmatic activity on the De Long Islands began. This stage was related to Miocene–Pliocene plume magmatism in the central part of the archipelago. The bulk of the volcanic pile of alkaline olivine basalts on Zhokhov Island was produced during the Late Miocene and Pliocene. The parental melts of these rocks had the same compositional characteristics as the melts that produced the within-plate basalts on Bennett Island. They were derived from a mantle source geochemically close to the reservoir that gave rise to the melts responsible for the Mesozoic within-plate magmatism in the northwestern termination of the De Long Islands. The alkaline basalt complex on Zhokhov Island was formed at relatively high degrees of melting, and the compositions of the rocks define fractionation trends typical of the picrite–alkaline basalt series of within-plate magmatism. When ascending to the surface, the magmatic melt from which the Zhokhov alkaline basalts crystallized entrained xenoliths of the ancient mantle material (spinel lherzolites and xenocrysts) and crustal rocks (quartzites, dolerites, and metavolcanic rocks). The "sampling" of different depth levels in the crust and mantle by the magmatic melt was, perhaps, made possible by the high degree of melting of the mantle source and the low velocity of magma ascent to the surface.

The same time span (Pliocene) was marked by the evelopment of a small volcanic edifice on Zhokhov Island. This edifice consisted of limburgites, i.e., within-plate volcanic rocks atypical of Mesozoic plume magmatism at the De Long Islands. Judging from their isotopic signatures, these alkaline volcanics were derived from the same mantle source as the alkaline olivine basalts accompanying these rocks but at lower (possibly, much lower) degrees of melting.

3. The youngest manifestations of plume magmatism on the De Long Islands were discovered only on the southernmost of the examined islands, on Vil'kitskii Island. The limburgites that possibly make up the whole island are of Pliocene age, their composition is close to that of the limburgites of Zhokhov Island, and they were derived from the same mantle source as that for the Zhokhov limburgite. At the same time, the limburgites from Vil'kitskii Island show some geochemical characteristics suggesting that they are more enriched within-plate rocks than the analogous volcanics of Zhokhov Island. This could be caused by a lower degrees of melting at which the parental melts of the Vil'kitskii limburgites were derived and a higher degree of enrichment of their mantle source. Neither the limburgites in Vil'kitskii Island nor these rocks in the central part of Zhokhov Island show evidence of significant fractionation and are, perhaps, the most primitive volcanic rocks of the De Long Islands. The limburgites in the central part of the archipelago and related alkaline olivine basalts contain numerous mantle xenoliths of spinel lherzolites. No crustal xenoliths were found in the limburgites on either Zhokhov or Vil'kitskii islands.

The scenario proposed above for the magmatic evolution in the De Long Islands implies that it was closely related to the activity of a plume mantle source situated beneath the continental shelf in the Laptev Sea and responsible for the pulses of magmatic activity in this part of the eastern sector of the Arctic basin over the past 124 m.y. In this context, it is expedient to compare the spatial distribution of the geochemical types of volcanic rocks of different ages over the De Long Islands with data on Late Quaternary volcanism in Northeast Asia (see the review in [*Grachev,* 1999]). As is pointed out in this publication, the most striking feature of Late Quaternary volcanism in this vast area is widespread within-plate magmatism, which occurred at all types of the crust (oceanic or continental). *Grachev* [1999] suggested that Quaternary magmatism in Northeast Asia (including the De Long Islands) was controlled by the melting of mantle plume material with its insignificant lithospheric contamination. The geodynamic environment of magmatism in the shelf zone of the Laptev Sea, which was influenced by the propagation of the Gakkel mid-oceanic ridge into the

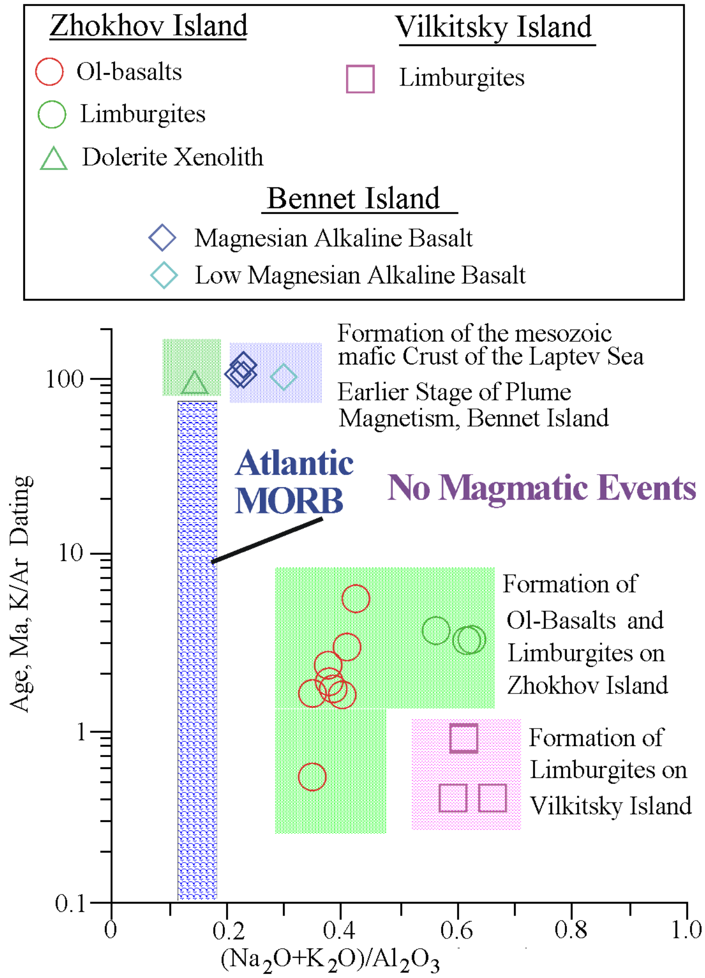

Figure 24. Compositional evolution of within-plate volcanism on the De Long Islands with time. See Figures 3 and 14 for symbol explanations.

shelf zone from the northwest, was referred to as pre-Afar [*Grachev,* 1999] and is thought to have corresponded to the early stages of the development of a mantle plume [*Grachev,* 1999].

The geodynamic style of magmatism of the De Long Islands makes it similar to magmatism in the Red Sea area, where the activity of two plumes (Afar at 45–0 Ma in the south and Levant–Nubian at 138–82 Ma in the north) predetermined the character of magmatism in the Red Sea Rift and north of it, along the Dead Sea and Jordan River valleys [*Segev,* 2000]. According to [*Segev,* 2000], these magmatic events were coupled with the extension of the continental lithosphere and the ascent of thermal anomalies corresponding to mantle plumes in the lower mantle. Thus, the development of rift zones in passive continental margins can be controlled by the ascent of one or several mantle plumes. It is worth noting that, according to [*Sharkov,* 2002], the northwestern part of the Arabian Peninsula (i.e., the area of the Levant–Nubian plume [*Segev,* 2000]) contains an association of Late Cenozoic within-plate volcanic rocks identical to the products of plume magmatism on the De Long Islands: alkaline basalts and basanites. As their within-plate analogues on Bennett and Vil'kitskii islands, these volcanic rocks, produced by magmatism triggered by the activity of a mantle plume and the opening of a young oceanic basin in the Red Sea area, bear mantle xenoliths of spinel lherzolites.

Compared with the magmatic complexes of the De Long Islands, the basaltoids in the Red Sea area are more heterogeneous chemically and comprise both oceanic tholeiites (including N-MORB), along with the acid derivatives of basaltoid magmatism (rhyolites and trachyandesites), and alkaline basalts [*Barrat et al.,* 1990, 1993; *Eissen et al.,* 1989; *Schilling,* 1969]. At the one hand, these differences could be caused by the more mature character of the spreading center in the Red Sea area, and, on the other hand, they could be controlled by kinematic factors. Indeed, magmatic complexes of the De Long Islands are compositionally similar to the plume-related rocks association in the northernmost part of the influence area of the Red Sea Rift, where there are no obvious traces of any oceanic spreading center (Levant–Nubian plume). According to [*Segev,* 2000], plume magmatism in this area becomes systematically younger from south to north starting from 244 Ma (Sinai) to 0.23 Ma (Golan Heights) or the Pleistocene (Shin and Syrian–Jordan plateaus [*Sharkov,* 2002]). Similar systematic variations in age are also typical of the volcanic products on the De Long Islands, where these variations are observed from northwest to southeast, from Bennett Island (124 Ma) to Vil'kitskii Island (0.4 Ma). It is pertinent to recall that, according to the data recently obtained in the course of the joint Russian–German seismic research in the Laptev Sea, its central part (in which we identified the youngest manifestations of plume magmatism) is marked by a Moho uplift [*Piskarev,* 2001].

Available data testify that the Red Sea spreading center, which controls the kinematics of lithospheric plates in the Middle East and West Asia, is characterized by extension velocities of about 1.6–2.2 cm/yr [*Dubinin and Ushakov,* 2001]. At the same time, the extension velocity in the greatest spreading zone of the Arctic Ocean, the Gakkel Ridge, near its intersection with the Laptev Sea shelf northwest of Bennett island is 0.7 cm/yr [*Michael et al.,* 2003]. Evidently, the geodynamics of the Gakkel Ridge (which belongs, according to [*Dick et al.,* 2003], to a new class of mid-oceanic ridges with ultraslow spreading) can significantly affect the style of the within-plate magmatism (first and foremost, the degree of melting and fractionation of the melts), which is related to its interaction with the lithosphere of the passive continental margin. Another distinctive feature of magmatism in this geodynamic environment is, perhaps, its very strong links with deep-seated enriched mantle sources and the absence of any indications that shallower DMM sources could have been involved in this process. Hence, the geochemical characteristics of magmatic products of the De Long Islands, which differentiate these rocks from magmatic associations in young fast-spreading rifts in passive continental margins, can be regarded as indirect arguments in support of the idea that the geological evolution of the continental shelf in the Laptev Sea was affected by the Gakkel mid-oceanic ridge propagating into this area.

Summarizing data on the magmatic complexes of the De Long Islands and related xenolith suite, it is logical to draw the conclusion that plume magmatism initiated rifting within the passive continental margin of the Laptev Sea shelf and served as a "conduit" for the spreading center propagating into this area. Another important outcome of our research is the conclusion that there is a certain dependence between the spreading velocity in a mid-oceanic ridge interacting with a passive continental margin and the geochemistry of magmatic rocks produced in this margin. It is possible that the geographic position of the mantle plume center determines the trajectory along which the mid-oceanic ridge penetrates into the passive continental margin and, thus, harbingers the development of a would-be divergent boundary of lithospheric plates in the distant future.

Acknowledgments. The authors thank L. A. Savostin (Shirshov Institute of Oceanology, Russian Academy of Sciences; LARGE), whose efforts made it possible to conduct successfully the Joint High-Latitude Expedition of Shirshov Institute of Oceanology and Vernadsky Institute of Geochemistry and Analytical Chemistry, Russian Academy of Sciences, in 1986 and 1988. The fieldwork on Zhokhov and Vil'kitskii islands was organized and carried out with the support of the administration of AANII and TUGS and the Director of the Polar Observatory on Zhokhov Island A. Kurygin. Samples of basalts from Bennett Island were made available for us by courtesy of G. B. Flerov and D. I. Golovin. The authors thank P. J. Michael and H. J. B. Dick for the recent fruitful discussion of the data used in this research. A keen and intense interest in our work was taken by A. F. Grachev, whose insistence made possible the appearance of this publication. This study was financially supported by the Russian Foundation for Basic Research, project no. 03-05-64018.

References

Aoki, K.(1984), Petrology of materials derived from the upper mantle, in *Materials Science of the Earth's Interior,* edited by I. Sunagawa, 415 pp., Terrapub, Tokyo.

Backlund, H. (1920), On the eastern part of the Arctic basalt plateau, *Med. Acad. Abo, Geol.-Mineral. Inst.,* 1, Abo.

Barrat, J. A., B. M. Jahn, S. Fourcade, and J. L. Joron (1993), Magma genesis in an ongoing rifting zone: the Tadjoura Gulf (Afar area), *Geochim. Cosmochim. Acta, 57,* 2291–2302.

Barrat, J.-A., B. M. Jahn, J. L. Joron, et al. (1990), Mantle heterogeneity in northeastern Africa: evidence from Nd isotopic compositions and hygromagmaphile element geochemistry of basaltic rocks from the Gulf of Tadjoura and southern Red Sea regions, *Earth Planet. Sci. Lett., 101,* 233–247.

Bogdanovskii, O. G., S. D. Mineev, S. S. Assonov, S. A. Silantyev, S. F. Karpenko, Yu. A. Shukolyukov, and L. A. Savostin (1992), Magmatism on the De Long Islands, eastern Arctic: isotopic geochemistry and geochronology, *Geokhimiya, 1,* 47–57.

Bogdanovskii, O. G., S. A. Silantyev, S. F. Karpenko, S. D. Mineev, and L. A. Savostin (1993), Ancient mantle xenoliths in young volcanic rocks on Zhokhov Island, De Long Islands, *Dokl. Russ. Akad. Nauk., 330,* 750–753.

Coombs, D. C., and J. F. G. Wilkinson (1969), Lineages and Fractionation trends in undersaturated rocks from the East Otago Volcanic Province, New Zealand, and related rocks, *J. Petrol., 10,* 440–501.

Dick, H. J. B., J. Lin, and H. Shouten (2003), An ultraslow-spreading class of ocean ridge, *Nature,*

Dosso, L., H. Bougault, C. Langmuir, et al. (1999), The age and distribution of mantle heterogeneity along the Mid-Atlantic Ridge (31°–41°N), *Earth Planet. Sci. Lett., 170,* 269–286.

Dubinin, E. P., and S. A. Ushakov (2001), *Oceanic riftogenesis,* 292 pp., GEOS, Moscow.

Eissen, J.-P., T. Juteau, J.-L. Joron, et al. (1989), Petrology and geochemistry of basalts from the Red Sea axial rift at 18° north, *J. Petrol., 30,* 791–839.

Fedorov, P. I., G. B. Flerov, and D. I. Golovin (2002), Volcanism on Bennett Island, East Arctic: new data on the composition and age of the rocks, in *School on the Geochemistry of Magmatic Rocks,* pp. 93–94, Vernadsky Institute of Geochemistry and Analytical Chemistry, Russ. Acad. Sci., Moscow.

Frey, F. A., and D. H. Green (1974), The mineralogy, geochemistry and origin of lherzolite inclusions in Victorian basanites, *Geochim. Cosmochim. Acta, 38,* 1023–1059.

Gakkel, Ya. Ya. (1957), *Science and Exploring of the Arctic,* 133 pp., Morskoi Transport, Leningrad.

Geology of the USSR (1984), vol. IX, 550 pp.

Geology of the USSR, Islands of the Soviet Arctic (1970), vol. XXVI, pp. 324–374.

Grachev, A. F. (1999), Quaternary volcanism and problems of geodynamics in Northeast Asia, *Fiz. Zemli, 9,* 19–37.

Hellebrand, E., J. E. Snow and R. Muhe (2002), Mantle melting beneath the Gakkel Ridge (Arctic Ocean): abyssal peridotite spinel composition, *Chem. Geol., 182,* 227–235.

Hofmann, A. W. (2003), Sampling mantle heterogeneity through oceanic basalts: isotopes and trace elements, in *Treatise on Geochemistry,* vol. 2, 61–101.

Ionov, D. A. (1988), Xenoliths in continental basalts, Ultramafic rocks of the earth's deep zones, in *Magmatic Rocks, Ultramafic Rocks,* pp. 311–332, Nauka, Moscow.

Ionov, D. A., and E. Jagoutz (1988), Sm and Nd isotopic composition of minerals in garnet and spinel peridotite xenoliths from the Vitim Highlands: the first data on mantle xenoliths in the USSR, *Doklady AN SSSR, 301,* 1195–1199.

Irving, A. J. (1980), Petrology and geochemistry of composite ultramafic xenoliths in alkalic basalts and implications for magmatic processes within the mantle, *Am. J. Sci., 280-A,* 389–426.

Jackson, E. D., and T. L. Wright (1970), Xenoliths in the Honolulu volcanic series, Hawaii, *J. Petrol., 11,* 405–430.

Kovalenko, V. I., D. A. Ionov, V. V. Yarmolyuk, E. Jagoutz, G. Lugmair, and H. G. Stosh (1990), Mantle evolution and its correlation with the crustal evolution in some areas in Central Asia: isotopic data, *Geokhimiya, 9,* 1308–1319.

Le Maitre, R. W. et al. (Eds.) (1989), *Classification of Igneous Rocks and Glossary of Terms, Part I, Recommendations of the International Union of Geological Sciences Subcommission on the Systematics of Igneous Rocks*, 150 pp. Blackwell, Oxford–London–Edinburgh–Boston–Melbourne.

Lindsley, D. H., and D. J. Anderson (1983), A two-pyroxene thermometer. Proc. Lunar Planet. Sci. Conf., Part 2: *J. Geophys. Res., 88A,* 887–906.

Mercier, J. C. (1980), Single-pyroxene thermobarometry, *Tectonophysics, 70,* 1–37.

Michael, P. J., C. H. Langmuir, H. J. B. Dick, J. E. Snow, S. L. Goldstein, D. W. Graham, K. Lehnert, G. Kurras, W. Jokat, R. Muhe, and H. N. Edmonds (2003), Magmatic and amagmatic seafloor generation at the ultraslow-spreading Gakkel Ridge, Arctic Ocean, *Nature, 423,* 956–961.

Mori, T., and D. H. Green (1978), Laboratory duplication of phase equilibria observed in natural garnet lherzolites, *J. Geol., 86,* 83–9.

Naryshkin, G. D. (1987), The mid-oceanic ridge of the Eurasian basin in the Arctic Ocean, in *The Results of Investigations Within the Scope of International Geophysical Projects,* 70 pp., Moscow.

O'Neill, H. St. C., and V. J. Wall (1987), The olivine–orthopyroxene–spinel oxygen geobarometer: the nickel precipitation curve and oxygen fugacity of the Earth's upper mantle, *J. Petrol., 28,* 1169–1193.

Piskarev, A. L. (2001), Sedimentation dynamics in the Laptev Sea as an indicator of changes in the spreading kinematics in the Eurasian basin of the Arctic Ocean, in *Geology and Geophysics of Mid-Oceanic Ridges, Trans. of S. P. Mashchenkov workshop of the Russian branch of the InterRidge international project,* p. 44, St. Petersburg.

Ringwood, A. E. (1975), *Composition and Petrology of the Earth's Mantle,* 570 pp., McGraw-Hill, New York–London–Toronto–Paris–Tokyo.

Sachtleben, Th., and H. A. Seck (1981), Chemical control of Al solubility in orthopyroxene and its implications for pyroxene geothermometry, *Contrib. Mineral. Petrol, 78,* 157–165.

Saggerson, E. P., and L. A. S. Williams (1964), Ngurumanite from southern Kenya and its bearing on the origin of rocks in the northern Tanganyika alkaline district, *J. Petrol., 5,* 40–81.

Savostin, L. A., S. A. Silantyev, and O. G. Bogdanovskii (1988), New data on volcanism at Zhokhov Island, De Long Islands, Arctic basin, *Doklady AN SSSR, 302,* 1443–1447.

Schilling, J.-G. (1969), Red Sea floor origin: rare-earth evidence, *Science, 165,* 1357–1360.

Segev, A. (2000), Synchronous magmatic cycles during the fragmentation of Gondwana: radiometric ages from the Levant and other provinces, *Tectonophysics, 325,* 257–277.

Sharkov, E. V. (2002), Interaction between the roof of a mantle plume and the earth crust during within-plate deformations: an example of the Late Cenozoic evolution of the Syrian territory, in *Int. symposium on mantle plumes and metallogeny,* pp. 285–287, Petrozavodsk–Moscow.

Silantyev, S. A., O. G. Bogdanovskii, and L. A. Savostin (2002), Geochemistry of within-plate oceanic rocks and related xenoliths in the central part of the De Long Islands as a clue to reconstructing the magmatic history of the Laptev Sea shelf, East Arctic basin, in *Int. symposium on mantle plumes and metallogeny,* pp. 223–225, Petrozavodsk–Moscow.

Silantyev, S. A., O. G. Bogdanovskii, L. A. Savostin, and N. N. Kononkova (1991), Magmatism at the De Long Islands, East Arctic: petrology and geochemistry of volcanic rocks and related xenoliths (Zhokhov and Vil'kitskii islands), *Geokhimiya, 2,* 267–277.

Sun, S.-S., and W. F. McDonough (1989), Chemical and isotopic systematics of oceanic basalts: implications for mantle composition and processes, in *Magmatism in Ocean Basins. Geol. Soc. Spec. Publ. London,* vol. 42, edited by A. D. Saunders and M. J. Norry, pp. 313–345.

Vaganov, V. I., and S. V. Sokolov (1988), *Thermobarometry of Mafic Mineral Assemblages,* 354 pp., Nedra, Moscow.

Vol'nov, D. A., and D. S. Sorokov (1961), Geology of Bennett Island, *Trans. Inst. Geol. Arktiki, Antarktiki, Akad. Nauk USSR, 123,* 25 pp.

Vol'nov, D. A., D. A. Voitsekhovskii, V. N. Voitsekhovskii, O. A. Ivanov, D. S. Sorokov, and D. S. Yashin (1970), New Siberian Islands, in *Geology of the USSR, Islands of the Soviet Arctic,* vol. XXVI, pp. 324–374.

Wass, S. Y. (1980), Geochemistry and origin of xenolith-bearing and related alkali basaltic rocks from the Southern Highlands, New South Wales, Australia, *Am. J. Sci., 280-A,* 639–666.

Wells, P. R. A. (1977), Pyroxene thermometry in simple and complex systems, *Contrib. Mineral. Petrol., 62,* 129–139.

Zhuravlev, A. Z., E. E. Laz'ko, and A. I. Ponomarenko (1991), Radiogenic isotopes and REE in minerals from garnet peridotite xenoliths in kimberlites of the Mir pipe, Yakutia, *Geokhimiya, 7,* 982–994.

Zindler, A., and S. Hart (1986), Chemical geodynamics, *Ann. Rev. Earth Planet. Sci., 14,* 439–571.

S. A. Silantyev, S. F. Karpenko, and Yu. A. Kostitsyn, Vernadsky Institute of Geochemistry and Analytical Chemistry, Russian Academy of Sciences, ul. Kosygina 19, Moscow, 119991 Russia

O. G. Bogdanovskii, Max-Plank-Institut für Chemie, Postfach 3060, D-55020 Mainz, Germany

P. I. Fedorov, Geological Institute, Russian Academy of Sciences, Pyzhevskii per. 7, Moscow, 109017 Russia

(Received 24 June 2004)